

# LEBANESE AMERICAN UNIVERSITY

Effect of permeability on the initiation of Atherosclerosis modeled  
as an inflammatory process

By  
Wissam C. El Hajj

A thesis  
Submitted in partial fulfillment of the  
requirements  
for the degree of Master of Science in  
Applied and Computational Mathematics

School of Arts and Science

June 2022

©2022

Wissam C. El Hajj

All Rights Reserved

## THESIS APPROVAL FORM

Student Name: Wissam El Hajj I.D. #: 201703256

Thesis Title: Effect of permeability on the initiation of Atherosclerosis modeled as an Inflammatory process

Program: Master of Applied and Computational Mathematics

Department: Computer Science and Mathematics

School: Arts and Sciences

The undersigned certify that they have examined the final electronic copy of this thesis and approved it in Partial Fulfillment of the requirements for the degree of:

Master in the major of Applied and Computational Mathematics

Thesis Advisor's Name: Nader El Khatib

Signature:  Date: 20 / 06 / 2022  
Day Month Year

Committee Member's Name: Chadi Nour

Signature:  Date: 20 / 06 / 2022  
Day Month Year

Committee Member's Name: Jean Takchi

Signature:  Date: 20 / 06 / 2022  
Day Month Year

## THESIS COPYRIGHT RELEASE FORM

### LEBANESE AMERICAN UNIVERSITY NON-EXCLUSIVE DISTRIBUTION LICENSE

By signing and submitting this license, you (the author(s) or copyright owner) grants the Lebanese American University (LAU) the non-exclusive right to reproduce, translate (as defined below), and/or distribute your submission (including the abstract) worldwide in print and electronic formats and in any medium, including but not limited to audio or video. You agree that LAU may, without changing the content, translate the submission to any medium or format for the purpose of preservation. You also agree that LAU may keep more than one copy of this submission for purposes of security, backup and preservation. You represent that the submission is your original work, and that you have the right to grant the rights contained in this license. You also represent that your submission does not, to the best of your knowledge, infringe upon anyone's copyright. If the submission contains material for which you do not hold copyright, you represent that you have obtained the unrestricted permission of the copyright owner to grant LAU the rights required by this license, and that such third-party owned material is clearly identified and acknowledged within the text or content of the submission. IF THE SUBMISSION IS BASED UPON WORK THAT HAS BEEN SPONSORED OR SUPPORTED BY AN AGENCY OR ORGANIZATION OTHER THAN LAU, YOU REPRESENT THAT YOU HAVE FULFILLED ANY RIGHT OF REVIEW OR OTHER OBLIGATIONS REQUIRED BY SUCH CONTRACT OR AGREEMENT. LAU will clearly identify your name(s) as the author(s) or owner(s) of the submission, and will not make any alteration, other than as allowed by this license, to your submission.

Name: **Wissam El Hajj**

Signature:



Date: **09 / 06 / 2022**

Day

Month

Year

## PLAGIARISM POLICY COMPLIANCE STATEMENT

I certify that:

1. I have read and understood LAU's Plagiarism Policy.
2. I understand that failure to comply with this Policy can lead to academic and disciplinary actions against me.
3. This work is substantially my own, and to the extent that any part of this work is not my own I have indicated that by acknowledging its sources.

Name: Wissam El Hajj

Signature: 

Date: 09 / 06 / 2022  
Day Month Year

To my future self.

## Acknowledgment

This dissertation would not have been achieved without the continuous guidance and support of several individuals whose assistance was priceless.

My sincere gratitude to Dr. Nader El Khatib for his dedication and precious encouragement. I am thankful for having the chance to work with such an amazing and professional advisor. He provided me constructive and efficient feedback at all stages of the research process

As well, I would like to thank the committee members, Dr. Jean Takchi and Dr. Chadi Nour for their commitment and guidance.

Also, I would like to express my special thanks to the Graduate program scholarship offered by the GSR office of the Lebanese American University for giving me this opportunity to work on this research thesis.

I extend my special thanks to my friend Ghada Abi Younes whose support and positive comments allowed me to enhance my research skills.

Moreover, another special thanks is dedicated for my family for always supporting me with love and trust. I would have never be able to accomplish any achievement nor results without their faith, encouragement and support. The daily prayers of my mother and father made me able to become the person I am today.

Finally, with all gratefulness, I expand my dedication to all my friends for their moral support and good will!

# Effect of permeability on the initiation of Atherosclerosis modeled as an inflammatory process

Wissam C. El Hajj

## Abstract

Atherosclerosis is an inflammatory chronic illness characterized by the buildup of fats, cholesterol and other substances in and on the artery wall causing its hardening. This work presents a mathematical model that analyze the inflammatory stage of atherosclerosis. We present a system of four coupled type of partial differential equations. Four leading players are taken into consideration: LDL ( $L$ ), oxidized LDL ( $Lox$ ), immune cells ( $M$ ) and the pro-inflammatory cytokines ( $C$ ). In addition, one characteristic parameter taken into account is the permeability of the endothelial layer.

$$\begin{cases} \frac{\partial L}{\partial t} = d_L \frac{\partial^2 L}{\partial x^2} + P(L_0 - L) - \lambda_L L \\ \frac{\partial Lox}{\partial t} = d_{Lox} \frac{\partial^2 Lox}{\partial x^2} + \alpha_L L - \alpha_{Lox} M Lox - \lambda_{Lox} Lox \\ \frac{\partial M}{\partial t} = d_M \frac{\partial^2 M}{\partial x^2} + \frac{P(C + \beta_1 Lox)}{1 + \frac{C}{\tau_1}} - \alpha_M M Lox - \lambda_M M \\ \frac{\partial C}{\partial t} = d_C \frac{\partial^2 C}{\partial x^2} + \frac{\alpha_2 M C}{1 + \frac{C}{\tau_2}} - \lambda_C C \end{cases}$$

A stability analysis and existence proof for fixed points of the kinetic system is presented leading to a biological interpretation. We are able to distinguish three main cases of the disease state that correlates with the permeability of the endothelial layer; where we can note that the permeability is classified according to its value based on the remaining parameters. In fact, when the permeability is low, this case is considered to be the disease free state since no chronic inflammatory reaction occurs due to the non initiation of the auto-amplification process. With intermediate permeability, a wave propagation corresponding to a chronic inflammatory reaction might happen, whether the initial perturbation overcome a threshold or not. With high permeability, even a small perturbation of the disease free state drives to a chronic inflammatory reaction represented by a wave propagation.

**Keywords:** Atherosclerosis, Partial Differential Equations, Mathematical Modelling, Permeability.

# Table of Contents

<b>List of Figures</b>	<b>x</b>
<b>List of Tables</b>	<b>xi</b>
<b>1 Biological and Mathematical Backgrounds</b>	<b>1</b>
1.1 Biological Process . . . . .	1
1.2 Literature review of various mathematical models of Atherosclerosis	4
<b>2 Proposed Model</b>	<b>7</b>
2.1 Description of the Proposed Model . . . . .	7
2.2 Mathematical analysis . . . . .	8
2.2.1 Kinetic System . . . . .	9
2.2.2 Equilibrium points . . . . .	9
2.3 Stability analysis . . . . .	12
2.3.1 Stability of $E_0$ . . . . .	12
2.3.2 Stability of $E_1$ . . . . .	12
2.3.3 Stability of $E_2$ and $E_3$ . . . . .	13
2.4 Bifurcation Analysis . . . . .	15
<b>3 Biological Interpretation</b>	<b>18</b>
<b>4 Existence and numerical simulations of travelling wave solutions</b>	<b>20</b>
4.1 Updated Model with $\alpha_{Lox} = \alpha_M = 0$ . . . . .	21
4.1.1 Equilibrium Points' Stability . . . . .	23
4.2 Complete model . . . . .	24
4.2.1 Perturbed Solution with $\alpha_M > 0$ and $\alpha_{Lox} = 0$ . . . . .	26
4.2.2 Perturbed Solution with $\alpha_M > 0$ and $\alpha_{Lox} > 0$ . . . . .	27
4.3 Numerical results . . . . .	28
<b>5 Discussion</b>	<b>32</b>
<b>Bibliography</b>	<b>34</b>

<b>Appendices</b>	<b>37</b>
<b>A Computations</b>	<b>38</b>
A.0.1 Detailed computation for the case presented in (2.2.2) . . .	38
<b>B Matlab Codes</b>	<b>41</b>

# List of Figures

1.1	Main worldwide causes of death [1]. . . . .	2
1.2	The atherogenesis process. . . . .	3
2.1	Case with one equilibrium point $E_1$ . . . . .	11
2.2	Case with three equilibrium points $E_1$ , $E_2$ and $E_3$ . . . . .	11
2.3	Case with two equilibrium points $E_1$ and $E_3$ . . . . .	12
2.4	Numerical convergence towards of the equilibrium points of the monostable case: $E_1$ is unstable and $E_3$ is stable. . . . .	14
2.5	Numerical convergence towards of the equilibrium points of the bistable case: $E_1$ and $E_3$ are stable, $E_2$ is unstable. . . . .	15
2.6	Bifurcation Diagram showing the stable points concentration of $M$ in function of the permeability $P$ . . . . .	16
2.7	Bifurcation Diagram showing the stable points concentration of $Lox$ in function of the permeability $P$ . . . . .	16
4.1	In case 1, a large perturbation of the the non-inflammatory state does not conduct to the propagation of a chronic inflammatory reaction. . . . .	29
4.2	In case 2, a large perturbation of the the non-inflammatory state does not lead to the propagation of a chronic inflammatory reaction. . . . .	29
4.3	In case 3.1, a small perturbation of the non-inflammatory state does not lead to the propagation of a chronic inflammatory reaction. . . . .	30
4.4	In case 3.2, a large perturbation of the non-inflammatory state leads to a wave propagation that corresponds to a chronic inflammatory reaction. . . . .	30
4.5	In case 4, even a small perturbation of the non-inflammatory state leads to a wave propagation that corresponds to a chronic inflammatory reaction. . . . .	31
A.1	Translation of condition 1 as function of $P$ . . . . .	39
A.2	Translation of condition 2 as function of $P$ . . . . .	39

# List of Tables

2.1	Choice of Parameters. . . . .	14
2.2	Stability of equilibrium points. . . . .	17

# Chapter 1

## Biological and Mathematical Backgrounds

### 1.1 Biological Process

Atherosclerosis is the main cause of cardiovascular diseases. Cardiovascular diseases form a group of illnesses that affect the heart and blood vessels. According to the latest statistics published by the World Health Organization, cardiovascular diseases are the leading cause of death worldwide. The number of people dying from cardiovascular diseases is alarming with more than 18.56 million death in 2019 [1]. Furthermore, we can note that in Lebanon, Heart diseases and strokes were the two leading causes of death between 2009 and 2019 [2]. Changing lifestyles and increasing life expectancy in countries experiencing an emerging economy, cardiovascular diseases' death rate tend to rise more there compared to already developed countries [3]. The main causes of such disease are mainly due to social performance of individuals, such as smoking, physical inactivity, excess consumption of alcohol and high saturated fat diets. Along with social behaviors, some risk factors are considered as physiological such as hypertension, high triglyceride and cholesterol levels. In the following part, we will be providing the biological mechanism behind atherosclerosis.

Atherosclerosis means hardening or thickening of an artery, due to the formation of a plaque, called atherosclerotic plaque. This plaque consists of a deposit of cholesterol, fatty substances and other substances which cause the narrowing of the artery and modification of the blood flow. This modification, is characterized by the restriction of blood flow to body organs which may lead in the course of time to strokes or heart attacks [4].

During the last decades, multiple studies focused on the pathogenesis of atherosclerosis, which is presumed to occur as a chronic inflammatory response to a layer

## Number of deaths by cause, World, 2019

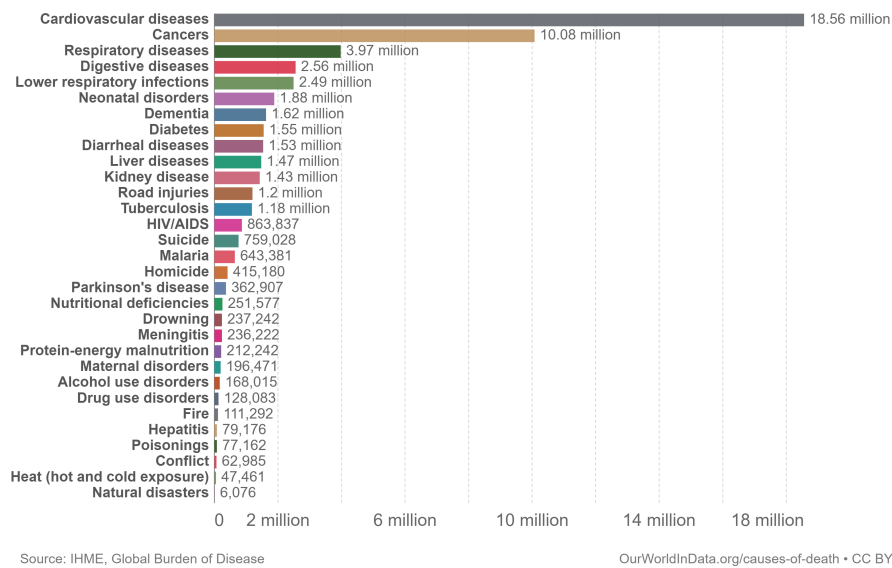


Figure 1.1: Main worldwide causes of death [1].

dysfunction in the arterial wall. The endothelial layer forms a boundary between the blood flowing in the lumen and the underlying tissues (see figure 1.2). The main responsibility of the vascular endothelium is homeostasis which consists of regulating transport of cells, nutrients and some necessary substances used for metabolic purposes [5]. Under laminar flow, homeostatic functions of the endothelium are activated, such as producing numerous constrictors and dilators substances, expressing some enzymes, favoring fibrinolysis. Furthermore, high shear stress boosts the production of nitric oxide (NO), one of the considerable vasodilator substance classified as relaxing factors derived by the endothelium and as an inhibitor to the oxidation of low-density lipoproteins (LDL) [6]. We can note here that a deficiency in the production or in the role of NO may lead to endothelium dysfunction.

The endothelium glycocalyx is a thick layer formed by glycoproteins and proteoglycans which is located on the luminal surface of the vascular endothelium wall [7]. One of the major functions of the glycocalyx is regulation of vascular permeability. Under disturbed flow, the thickness of the glycocalyx is reduced especially in atherosclerotic areas, which weakens its function as a barrier and favors access for low density lipoproteins (LDL) to the arterial intima [8]. Thus, smooth laminar flow protects the glycocalyx, boosts the production of NO and limits the access for LDL particles to enter the arterial intima. Based on clinical studies, it is approved that due to many behavioral and physiological risk factors, the endothelium wall becomes dysfunctional, which in return is classified as the first step of the atherosclerosis process [9].

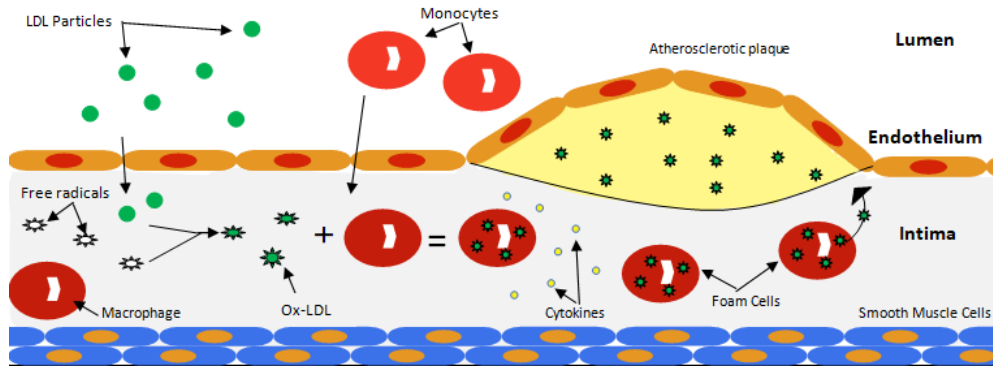


Figure 1.2: The atherogenesis process.

High plasma concentration of LDL is the main risk factor behind atherosclerosis. Because of endothelium dysfunction, permeability of the endothelial wall increases so that many particles travelling in the blood might access the arterial intima such as LDL particles. Once LDL penetrates into the arterial intima, they are prone to oxidation due to the presence of free radicals such as peroxy radicals which are issued from chemical reactions, and they are called as oxidized-LDL (ox-LDL) [4]. It is generally agreed that this alteration in LDL is labeled as one of the earliest steps in the atherosclerotic process. The immune system considers oxidized LDL as a foreign particle and it should be removed. Hence, an immune response is launched and chemoattractants are released and endothelium cells are activated to let the white blood cells (Monocytes) bond to the wall and penetrate into the inner lining of the artery that is the intima [10]. Then, monocytes are converted into macrophages so that they phagocytose ox-LDL. The process of phagocytose of ox-LDL is complex, but can be simplified to the following: once ox-LDL molecules are engulfed by macrophages, they are catabolized and they undergo a partial structure disruption [11]. This process leads to intra-cellular accumulation of cholesterol which will turn macrophages into foam cells.

Foam cells are also considered dangerous by our immune system and should be removed. Hence, pro-inflammatory cytokines are released which will again activate the endothelium cell in order to promote the enrollment of more monocytes which will cause in return the production of new pro-inflammatory cytokines. However, oxidation of more LDL particles will cause the enrollment of more monocytes that will induce the amplification of the inflammatory response. The phenomenon explained previously is called an auto-amplification process and is balanced by an anti-inflammatory phenomenon which will release anti-inflammatory cytokines. We can note here that anti-inflammatory macrophages releases anti-inflammatory cytokines which in return will prohibit the production of pro-inflammatory cytokines. As a result, foam cells are not affected by degradation which restrict their neutralization by the immune system[11]. Thus, in order to promote stabilization

of the lipid accumulation, foam cells secrete growth factors in order to stimulate the proliferation and migration of smooth muscle cells to create a fibrous cap over the lipid deposit. Gradually with respect to time, the lipid deposit harden and becomes more compact which stimulates the formation of a plaque.

The plaque formation is classified as one of the progressive stages of atherosclerosis. As a matter of fact, the fibrous cap alters the geometry of the artery and interacts with the blood flow. Once the formation is done, scientists distinguished two type of plaque between stable and unstable. For example, when the fibrous cap is considered hard along with a poor lipid core, the plaque is stable and is unlikely to undergo rupture. In opposition to unstable plaque, also called vulnerable plaques, that are prone to rupture and their fibrous cap is considered to be thin along with a significant lipid core. Subsequently, it may after some period of time undergo rupture and may cause numerous deadly coronary syndromes [12]. Multiple studies have been examining how the endothelium dysfunction might be restored. In addition, we can note that targeting the increase in permeability of the endothelium layer can be considered as an encouraging method to prevent inflammation and atherosclerosis. Moreover, numerous interventions like lipid-lowering therapy, healthy diets and routine physical activity have been evaluated effective [6]. Furthermore, we can note that many pharmacological studies have focused on the regulation of the glycocalyx degradation, yet additional analysis are required [8]. Finally, we can highlight that permeability of the endothelium layer plays a major role in the initial phase of the atherogenesis mechanism.

## **1.2 Literature review of various mathematical models of Atherosclerosis**

Mathematical modelling refers to the process of creating a mathematical depiction of a real-world problem to make a forecast or provide insights. It provides a research tool to develop scientific interpretation and analysis applied on many major disciplines, specifically in the biomedical field. For the last decades, many models of atherosclerosis have been developed, using various modelling techniques.

Many models have taken into account the first step in the atherosclerotic process that is the penetration of LDL molecules circulating in the blood to the arterial intima. For example, in [13] the LDL concentration distribution near the endothelium layers is directly linked to the geometry of the artery. It is generally agreed that in regions of low shear stress we have an increase in the accumulation of LDL molecules near the wall. In region of high shear stress, no accumulation of LDL molecules occurs, in contrast to regions of low flow occurring in the bifur-

cation regions [13].

Many mathematical models have studied different stages of atherosclerosis like the effect of risk factors, the plaque formation or fluid structure interaction between the plaque and blood. For example, in [14], authors presented a kinetic model for the oxidation of LDL molecules within the arterial intima. The kinetic model is used in a reaction-diffusion equation for modelling the role of LDL transport into the arterial wall. Moreover, results highlighted the fact that the constant of LDL oxidation plays a major role in the LDL concentration accumulation in the intima. Importance of LDL oxidation rate can be correlated to the concentration of oxidized LDL in the intima. The following correlation is studied in [10]. In fact, authors presented a study on the inflammatory process of the development of atherosclerosis in a one and two dimensional model of reaction-diffusion system type, where concentration of immune cells and cytokines are taken into account. In addition, the major parameter of the model is considered the ox-LDL concentration in the arterial intima [10]. Low ox-LDL concentration corresponds to a disease free state. In opposition to a relative high concentration where a small perturbation of the non-inflammatory state leads to a chronic inflammatory reaction response represented by a travelling wave propagation, this case is called monostable. Whereas, an intermediate concentration of oxidized LDL guides to a bistable case where a chronic inflammatory reaction may set up depending on whether the perturbation is large enough so that the threshold is overcome. Similarly, authors in [15] advanced a two-dimensional model of the development and initiation of the atherosclerotic process in a system of type reaction-diffusion by taking into account same concentrations in the arterial intima. However, the domain is illustrated as a 2D-strip where the recruitment of immune cells as a function of cytokines' concentration is considered a boundary condition and existence of travelling waves is proved.

The work presented in [11] considers the concentration of ox-LDL in addition to the concentrations of immune cells and cytokines as in [10]. Results obtained are similar but divided into seven possible cases, thus it can be considered more realistic. In addition, [11] showed the role and effect of HDL (High density lipoproteins) on the plaque formation, where three different regions are recognized and classified between low risk, high risk and stabilized inflammation regions. Thus, we can note that HDL along with LDL are molecules that play a major role in determining the risk of atherosclerosis. For example, in [16] authors explored a mathematical model that models the formation of a plaque where thirteen parameters are taken into account like LDL, HDL, free radicals, foam cells, ox-LDL, immune cells. The presented model consists of a system of partial differential equations and numerical simulations are performed using various concentration

of LDL and HDL in blood in order to determine whether an atherosclerotic plaque grows or disappears.

The role of permeability of the endothelial layer in the initiation of atherosclerosis is important. For example, in [17] authors suggested a model of fourteen partial differential equations of reaction-diffusion type that model the concentrations of various parameters such as LDL, HDL, free radicals, ox-LDL, immune cells and cytokines. The effect of permeability is introduced in the recruitment of monocytes, low and high density lipoproteins and T-helper cells. Also, permeability is defined to be a function of ox-LDL and cytokines produced by macrophages. After proving the existence of travelling wave solutions for a reduced model, numerical simulations are performed for the complete model to show various results such as the regulation role of anti-inflammatory cytokines. We can note that various mathematical models are used to model the blood flow in addition to the concentrations of various parameters and the permeability of the endothelial layer. In [18], authors proposed a model formed by partial differential equations, where Navier-Stokes equations models the blood flow, Biot equations describe the fluid flow inside the vessel wall that is defined as pro-elastic and convection/chemotaxis-reaction-diffusion equations to model transport, signaling and interaction process for the development of an inflammation and atherosclerosis. The domain was taken as a two-dimensional geometry in order to study the role of endothelial permeability. Numerical simulations show that the prediction of potential locations of atherosclerotic plaques is not only related to wall shear stress, since the endothelial permeability is strongly affected by many other factors such as monocyte chemoattractants.

Many mathematical models presented the role of many parameters however no model can distinguish between all of them because of the high number of risk factors. Paper [19] explores various stages of atherosclerosis in a spatial and non-spatial ways. In all stages presented, the blood is considered to be a newtonian fluid along with a known velocity. The penetration of lipoproteins to the intima and their oxidation along with the inflammatory process activated by immune cells are all presented.

In the next chapter, we propose a model that is inspired from various references by taking into consideration some modelling techniques along with modifications.

# Chapter 2

## Proposed Model

### 2.1 Description of the Proposed Model

We present the following mathematical model which models the set up of an atherosclerotic inflammatory reaction on an interval representing the arterial intima. The model takes into account the following contributors to the inflammatory process: the immune cells (monocytes and macrophages), LDL, oxidized LDL and cytokines.

Four coupled partial differential equations form the system. All differential equations are of reaction-diffusion type for  $x \in [0, \infty[$  and  $t \in [0, \infty[$ . In addition, we impose homogeneous Neumann boundary conditions at the boundaries.

$$\frac{\partial L}{\partial t} = d_L \frac{\partial^2 L}{\partial x^2} + P(L_0 - L) - \lambda_L L, \quad (2.1)$$

$$\frac{\partial Lox}{\partial t} = d_{Lox} \frac{\partial^2 Lox}{\partial x^2} + \alpha_L L - \alpha_{Lox} M Lox - \lambda_{Lox} Lox, \quad (2.2)$$

$$\frac{\partial M}{\partial t} = d_M \frac{\partial^2 M}{\partial x^2} + \frac{P(C + \beta_1 Lox)}{1 + \frac{C}{\tau_1}} - \alpha_M M Lox - \lambda_M M, \quad (2.3)$$

$$\frac{\partial C}{\partial t} = d_C \frac{\partial^2 C}{\partial x^2} + \frac{\alpha_2 M C}{1 + \frac{C}{\tau_2}} - \lambda_C C. \quad (2.4)$$

$L$  represents the concentration of LDL,  $Lox$  the concentration of ox-LDL,  $M$  the concentration of immune cells and  $C$  the concentration of cytokines.

We assume that all the parameters present in the above system are positive.

Equation (2.1) expresses the change of the concentration of LDL in time within arterial intima. The term  $d_L \frac{\partial^2 L}{\partial x^2}$  corresponds to the diffusion of LDL. The term  $P(L_0 - L)$  represents the beginning of the atherosclerotic process that is the penetration of LDL from the lumen into the intima due to the action of the per-

meability  $P$ .

Equation (2.2) expresses the change of the concentration of ox-LDL in time within the arterial intima. The term  $d_{Lox} \frac{\partial^2 Lox}{\partial x^2}$  corresponds to the diffusion of ox-LDL. The source term  $\alpha_L L$  describes the oxidation of LDL particles. The term  $-\alpha_{Lox} M Lox$  describes the phagocytosis process, where macrophages phagocytose ox-LDL molecules which will cause macrophages to transform into foam cells.

Equation (2.3) expresses the evolution in time of the concentration of immune cells denoted by  $M$  within the arterial intima. The term  $d_M \frac{\partial^2 M}{\partial x^2}$  corresponds to the diffusion of  $M$ . The term  $\frac{P(C+\beta_1 Lox)}{1+C\tau_1}$  describes the recruitment of monocytes from the lumen to the arterial intima due to the presence of pro-inflammatory cytokines and ox-LDL. The term  $P\beta_1 Lox$  describes the recruitment of monocytes due to the presence of ox-LDL, which are considered harmful by our immune system. The term  $PC$  describes the auto-amplification of the recruitment of monocytes due to the presence of pro-inflammatory cytokines. We can note, that the term  $P$  (permeability of endothelium layer) plays a major role in the recruitment of monocytes. The term  $1 + \frac{C}{\tau_1}$  expresses the mechanical saturation of the enrollment of  $M$ . In fact, it describes the effect of the fibrous cap created by smooth muscle cells, with  $\tau_1$  representing the time needed for the formation of the fibrous cap. The phagocytose process of oxidized LDL by Macrophages is described by the term  $-\alpha_M M Lox$ .

Equation (2.4) expresses the evolution in time of the concentration of  $C$  (cytokines) within the arterial intima. The term  $d_C \frac{\partial^2 C}{\partial x^2}$  corresponds to the diffusion of  $C$ . The presence of macrophages in the arterial intima promotes the production of pro-inflammatory cytokines. It is modeled by the term  $\frac{\alpha_2 M C}{1 + \frac{C}{\tau_2}}$ , where  $\alpha_2 C$  models the secretion of cytokines promoted by the cytokines themselves. The term  $1 + \frac{C}{\tau_2}$  models the inhibition of the secretion of pro-inflammatory cytokines interfered by the anti-inflammatory cytokines, with  $\tau_2$  representing the needed time for inhibition to act.

The last term of equations (2.1)-(2.4) describe the degradation rate of their respective substance.

## 2.2 Mathematical analysis

In this part, we study existence and stability of equilibrium points of the kinetic system of system (2.1)-(2.4).

## 2.2.1 Kinetic System

The kinetic system of (2.1)-(2.4) reads:

$$\begin{cases} \frac{dL}{dt} = P(L_0 - L) - \lambda_L L, \\ \frac{dLox}{dt} = \alpha_L L - \alpha_{Lox} MLox - \lambda_{Lox} Lox, \\ \frac{dM}{dt} = \frac{P(C + \beta_1 Lox)}{1 + \frac{C}{\tau_1}} - \alpha_M MLox - \lambda_M M, \\ \frac{dC}{dt} = \frac{\alpha_2 MC}{1 + \frac{C}{\tau_2}} - \lambda_C C. \end{cases} \quad (2.5)$$

## 2.2.2 Equilibrium points

**Definition 2.2.1.** Equilibrium points of an autonomous system of the form  $\frac{dY}{dt} = F(Y)$  are attained by solving the system  $F(Y) = 0$ .

We use by the upper script \* for the components of the equilibrium points. In order to determine the fixed points of system (2.5), we solve:

$$\begin{cases} P(L_0 - L) - \lambda_L L = 0, \\ \alpha_L L - \alpha_{Lox} MLox - \lambda_{Lox} Lox = 0, \\ \frac{P(C + \beta_1 Lox)}{1 + \frac{C}{\tau_1}} - \alpha_M MLox - \lambda_M M = 0, \\ \frac{\alpha_2 MC}{1 + \frac{C}{\tau_2}} - \lambda_C C = 0. \end{cases} \quad (2.6)$$

We can distinguish two cases: a case where  $P = 0$  and a case where  $P \neq 0$ .

### Case of zero permeability

If  $P = 0$ , the system (2.6) becomes:

$$\begin{cases} \lambda_L L = 0, \\ \alpha_L L - \alpha_{Lox} MLox - \lambda_{Lox} Lox = 0, \\ -\alpha_M MLox - \lambda_M M = 0, \\ \frac{\alpha_2 MC}{1 + \frac{C}{\tau_2}} - \lambda_C C = 0. \end{cases} \quad (2.7)$$

We get  $L^* = 0$ ,  $M^* = 0$ ,  $Lox^* = 0$  and  $C^* = 0$ . Then the equilibrium point in this case is  $E_0 = (L^*, Lox^*, M^*, C^*) = (0, 0, 0, 0)$

### Case of non-zero permeability

If  $P \neq 0$ , we get back to system (2.6) :

$$\begin{cases} P(L_0 - L) - \lambda_L L = 0, \\ \alpha_L L - \alpha_{Lox} M Lox - \lambda_{Lox} Lox = 0, \\ \frac{P(C + \beta_1 Lox)}{1 + \frac{C}{\tau_1}} - \alpha_M M Lox - \lambda_M M = 0, \\ \frac{\alpha_2 M C}{1 + \frac{C}{\tau_2}} - \lambda_C C = 0. \end{cases}$$

After solving the first equation we get  $L^* = \frac{PL_0}{P + \lambda_L}$ . The fourth equation of (2.6), leads to either  $C = 0$  or  $M = \frac{\lambda_C}{\alpha_2} \left(1 + \frac{C}{\tau_2}\right)$ .

**Nullclines on the hyperplane  $C=0$ .** For  $C = 0$  and  $L^* = \frac{PL_0}{P + \lambda_L}$ , the remaining two equations leads to the system:

$$\begin{cases} M = f_1(Lox) := \frac{\alpha_L L^* - \lambda_{Lox} Lox}{\alpha_{Lox} Lox}, \\ M = f_2(Lox) := \frac{P\beta_1 Lox}{\alpha_M Lox + \lambda_M}. \end{cases} \quad (2.8)$$

The possible intersection between  $f_1$  and  $f_2$  in the positive plane is one equilibrium point  $E_1 = (L^*, Lox^*, M^*, 0)$ . Furthermore, we can note that  $Lox^* = \frac{(\alpha_L \alpha_M L^* - \lambda_M \lambda_{Lox}) + \sqrt{\kappa}}{2(\alpha_M \lambda_{Lox} + P \alpha_{Lox} \beta_1)}$  and  $M^* = \frac{P \beta_1 Lox^*}{\alpha_M Lox^* + \lambda_M}$ , where  $\kappa = (\alpha_L \alpha_M L^* - \lambda_M \lambda_{Lox})^2 + 4 \lambda_M \alpha_L L^* (\alpha_M \lambda_{Lox} + P \alpha_{Lox} \beta_1)$ .

**Nullclines on the hyperplane  $M = \frac{\lambda_C}{\alpha_2} \left(1 + \frac{C}{\tau_2}\right)$ .** Similarly, in this case we have  $L^* = \frac{PL_0}{P + \lambda_L}$ . From the second equation of system, we get:  $Lox = \frac{\alpha_L L^*}{\alpha_{Lox} M + \lambda_{Lox}}$ . Then the third equation turns into a second order polynomial in function of  $M$ :

$$\lambda_M \left(1 + \frac{C}{\tau_1}\right) \alpha_{Lox} M^2 - \gamma M - PC \lambda_{Lox} - P \beta_1 \alpha_L L^* = 0 \quad (2.9)$$

where  $\gamma = (PC \alpha_{Lox} - \alpha_M \alpha_L L^* \left(1 + \frac{C}{\tau_1}\right) - \lambda_M \lambda_{Lox} \left(1 + \frac{C}{\tau_1}\right))$

Solving equation (2.9), we obtain:

$$\Delta = (PC \alpha_{Lox} - \alpha_M \alpha_L L^* \left(1 + \frac{C}{\tau_1}\right) - \lambda_M \lambda_{Lox} \left(1 + \frac{C}{\tau_1}\right))^2 + 4 \alpha_{Lox} \lambda_M \left(1 + \frac{C}{\tau_1}\right) (PC \lambda_{Lox} + P \beta_1 \alpha_L L^*)$$

$$M = \frac{(PC\alpha_{Lox} - \alpha_M\alpha_L L^*(1 + \frac{C}{\tau_1}) - \lambda_M\lambda_{Lox}(1 + \frac{C}{\tau_1})) + \sqrt{\Delta}}{2\lambda_M\alpha_{Lox}(1 + \frac{C}{\tau_1})}$$

Combining both solutions for  $M$ , we derive the following system :

$$\begin{cases} M=g_1(C) := \frac{(PC\alpha_{Lox}-\alpha_M\alpha_L L^*(1+\frac{C}{\tau_1})-\lambda_M\lambda_{Lox}(1+\frac{C}{\tau_1}))+\sqrt{\Delta}}{2\lambda_M\alpha_{Lox}(1+\frac{C}{\tau_1})}, \\ M=g_2(C) := \frac{\lambda_C}{\alpha_2}(1 + \frac{C}{\tau_2}). \end{cases} \quad (2.10)$$

Equating  $g_1 = g_2$ , we get three possible cases for the intersection between the curve  $g_1$  and the line  $g_2$ . The first case is where no positive intersection between the two curves. The second case is where we get two intersection points in the positive plane, so that we can deduce the existence of two equilibrium points denoted by  $E_2$  and  $E_3$ . The last case is where the curves intersect in one point in the positive plane leading to one fixed point denoted by  $E_3$ .

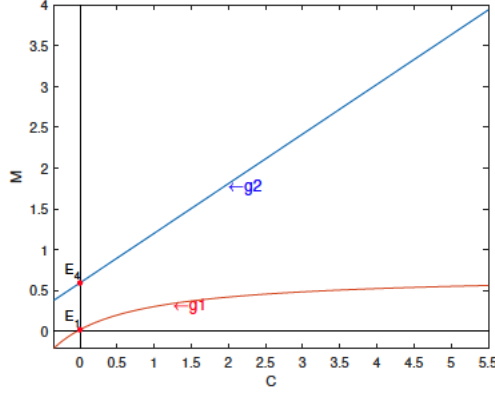


Figure 2.1: Case with one equilibrium point  $E_1$ .

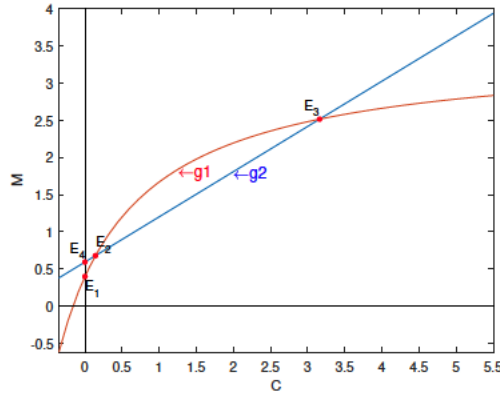


Figure 2.2: Case with three equilibrium points  $E_1$ ,  $E_2$  and  $E_3$ .

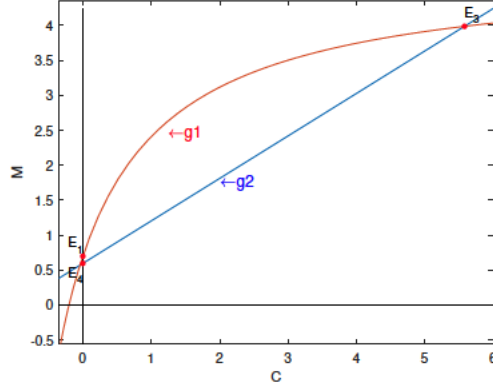


Figure 2.3: Case with two equilibrium points  $E_1$  and  $E_3$ .

## 2.3 Stability analysis

In this part, the stability of the found equilibrium points  $E_0$ ,  $E_1$ ,  $E_2$  and  $E_3$ , when they exist, is studied. Mathematically, stability of a fixed point can be found analytically or numerically. In this analysis, the stability of  $E_0$  and  $E_1$  will be performed analytically.

We denote by  $J$  the Jacobian matrix of system (2.5) :

$$J = \begin{pmatrix} -P - \lambda_L & 0 & 0 & 0 \\ \alpha_L & -\alpha_{Lox}M - \lambda_{Lox} & -\alpha_{Lox}Lox & 0 \\ 0 & -\alpha_M M + \frac{P\beta_1}{1+\frac{C}{\tau_1}} & -\alpha_M Lox - \lambda_M & \frac{P - \frac{P\beta_1 Lox}{\tau_1}}{(1+\frac{C}{\tau_1})^2} \\ 0 & 0 & \frac{\alpha_2 C}{1+\frac{C}{\tau_2}} & \frac{\alpha_2 M}{(1+\frac{C}{\tau_2})^2} - \lambda_C \end{pmatrix}$$

Denote by  $J_{E_i}$  the Jacobian matrix applied at the equilibrium point  $E_i$

### 2.3.1 Stability of $E_0$

Recall that  $E_0 = (0, 0, 0, 0)$ . We get  $J_{E_0} = \begin{pmatrix} -\lambda_L & 0 & 0 & 0 \\ \alpha_L & -\lambda_{Lox} & 0 & 0 \\ 0 & 0 & -\lambda_M & 0 \\ 0 & 0 & 0 & -\lambda_C \end{pmatrix}$

We get the following eigenvalues of  $J_{E_0}$ :  $-\lambda_L$ ,  $-\lambda_{Lox}$ ,  $-\lambda_M$  and  $-\lambda_C$ , which are all strictly negative. Thus,  $E_0$  is a stable equilibrium point.

### 2.3.2 Stability of $E_1$

Recall that  $E_1 = (\frac{PL_0}{P+\lambda_L}, Lox^*, M^*, 0)$  with

$$Lox^* = \frac{(\alpha_L \alpha_M L^* - \lambda_M \lambda_{Lox}) + \sqrt{\theta}}{2(\alpha_M \lambda_{Lox} + P \alpha_{Lox} \beta_1)}$$

where  $\theta = (\alpha_L \alpha_M L^* - \lambda_M \lambda_{Lox})^2 + 4\lambda_M \alpha_L L^* (\alpha_M \lambda_{Lox} + P \alpha_{Lox} \beta_1)$   
and  $M^* = \frac{P \beta_1 Lox^*}{\alpha_M Lox^* + \lambda_M}$ .

We obtain the following Jacobian matrix:

$$J_{E_1} = \begin{pmatrix} -P - \lambda_L & 0 & 0 & 0 \\ \alpha_L & -\alpha_{Lox^*} M^* - \lambda_{Lox} & -\alpha_{Lox} Lox^* & 0 \\ 0 & -\alpha_M M^* + P \beta_1 & -\alpha_M Lox^* - \lambda_M & P - \frac{P \beta_1 Lox^*}{\tau_1} \\ 0 & 0 & 0 & \alpha_2 M^* - \lambda_C \end{pmatrix}$$

To find the eigenvalues of  $J_{E_1}$ , we solve:  $|J_{E_1} - \lambda I| = 0$ , where  $\lambda$  being an eigenvalue of  $J_{E_1}$ . We get:

$$(-P - \lambda_L - \lambda)(\alpha_2 M^* - \lambda_C - \lambda) \begin{vmatrix} -\alpha_{Lox} M^* - \lambda_{Lox} - \lambda & -\alpha_{Lox} Lox^* \\ -\alpha_M M^* - P \beta_1 & -\alpha_M Lox^* - \lambda_M - \lambda \end{vmatrix} = 0$$

We get  $\lambda_1 = -P - \lambda_L < 0$  and  $\lambda_2 = \alpha_2 M^* - \lambda_C$ .

Proceeding with the remaining 2 by 2 determinant we get:

$$\lambda^2 + \lambda[M^* \alpha_{Lox} + \lambda_{Lox} + \alpha_M Lox + \lambda_M] + \lambda_M \alpha_{Lox} M^* + \alpha_M \lambda_{Lox} Lox^* + \lambda_{Lox} \lambda_M + \alpha_{Lox} P \beta_1 Lox^* = 0$$

A Sum-Product analysis for the roots of the second degree polynomial is performed. We get that  $\lambda_3$  and  $\lambda_4$  have both negative real part. Leading us back to  $\lambda_2 = \alpha_2 M^* - \lambda_C$ , where we can deduce that  $E_1$  is stable where  $M^* < \frac{\lambda_C}{\alpha_2}$  and unstable otherwise. In the  $C - M$  plane we can get the following graphical interpretation : if  $E_1 = (0, M^*)$  is situated below  $E_4 = (0, \frac{\lambda_C}{\alpha_2})$ ,  $E_1$  is stable. In opposition, if  $E_1 = (0, M^*)$  is situated above  $E_4 = (0, \frac{\lambda_C}{\alpha_2})$ ,  $E_1$  is unstable.

### 2.3.3 Stability of $E_2$ and $E_3$

Here, the stability of the equilibrium points  $E_2$  and  $E_3$  when they exist is studied. Recall the three cases obtained on existence of equilibrium points: The first case is where only  $E_1$  exists, which can be stable or unstable. The second case, also called the Bistable case, is where we get the existence of two stationary points denoted by  $E_2$  and  $E_3$ . The third case, also called the Monostable Case, is where we get one fixed point denoted by  $E_3$ .

Value	Reference
$L_0=1.9 \text{ mg.cm}^{-3}$	[18]
$\lambda_C =1.188\text{day}^{-1}$	[17]
$\lambda_{Lox}= 2.0736\text{day}^{-1}$	[17]
$\alpha_L=1.4 \cdot 10^{-4}\text{s}^{-1} = 12.096\text{day}^{-1}$	[14]
$\lambda_L= 12.096\text{day}^{-1}$	Assuming all dead LDL are converted into ox-LDL
$\alpha_{Lox}= 0.01$	estimated
$\alpha_M= 0.0120096$	estimated
$\lambda_M= 1.9872$	estimated
$\tau_1= 1.4$	estimated
$\tau_2= 42/43$	estimated
$\alpha_2= 2$	estimated
$\beta_1= 0.05$	estimated

Table 2.1: Choice of Parameters.

We show the stability of the equilibrium points  $E_2$  and  $E_3$  using numerical simulations with considering the values of all parameters taken as in Table (2.1).

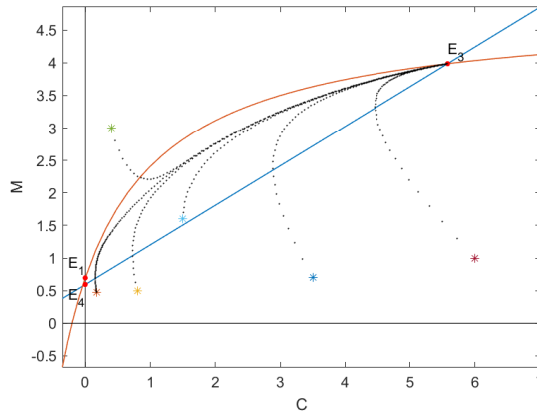


Figure 2.4: Numerical convergence towards of the equilibrium points of the monostable case:  $E_1$  is unstable and  $E_3$  is stable.

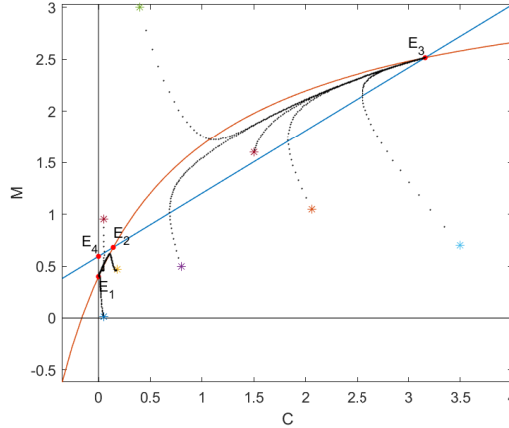
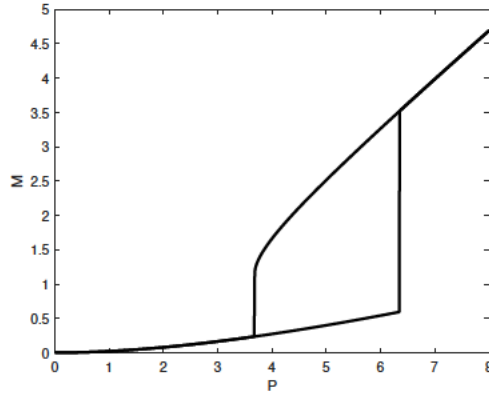


Figure 2.5: Numerical convergence towards of the equilibrium points of the bistable case:  $E_1$  and  $E_3$  are stable,  $E_2$  is unstable.

## 2.4 Bifurcation Analysis

A bifurcation diagram is a visual description of the relationship between the value of one parameter (the permeability in our case) and the critical points' behavior. In this section, we consider the permeability  $P$  as the varying parameter and the values to the stable equilibrium points concentrations of  $M$  in the first step and  $Lox$  in a further step.

In order to perform an analysis on the permeability  $P$ , the only parameter we did not impose a fixed value, we have opted for a Bifurcation diagram. All remaining values are given as in table (2.1). The diagram illustrates the concentration of immune cells of the fixed points that are stable versus the permeability. As a result shown in the figure below, we can highlight that for a low permeability, we only get existence of  $E_1$  which is stable, for an intermediate permeability we get existence of two fixed points  $E_1$  and  $E_3$  being stable and  $E_2$  being unstable, and for a high permeability, we get the existence of  $E_1$  being unstable and  $E_3$  being stable.



**Figure 2.6:** Bifurcation Diagram showing the stable points concentration of  $M$  in function of the permeability  $P$ .

This diagram correlates with the results obtained in the computation on existence and stability of the equilibrium points.

In addition, we have obtained the following bifurcation diagram showing the stable points concentration of  $Lox$  in function of the permeability  $P$ . Again, here we can highlight that the diagram correlates with the analytic existence and stability of the equilibrium points. Note here that we have used the same values for parameters as in Table (2.1) except for  $\beta_1 = 0.25$ ,  $\alpha_{Lox} = 8$  and  $\alpha_M = 0.120096$ .

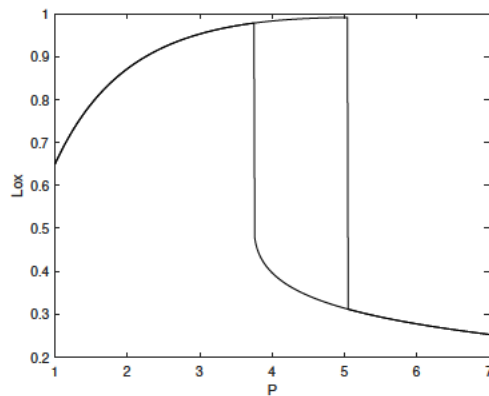


**Figure 2.7:** Bifurcation Diagram showing the stable points concentration of  $Lox$  in function of the permeability  $P$ .

As a recapitulation, we summarize the cases in the following table:

Permeability P	0	Low	Intermediate	High
$E_0$	stable	-	-	-
$E_1$	-	stable	stable	unstable
$E_2$	-	-	unstable	-
$E_3$	-	-	stable	stable

Table 2.2: Stability of equilibrium points.

# Chapter 3

## Biological Interpretation

In this chapter, we present a biological interpretation of the equilibrium points.

- $E_0$  is the equilibrium point corresponding to a zero-permeability. In other words, no LDL particles, not immune cells can penetrate into the arterial intima. As a result, no production of ox-LDL nor cytokine can be made. It corresponds to the case where no interaction between the lumen and the arterial intima, then no inflammation reaction set up is possible in this case. This equilibrium is stable as proved in section 2.3.
- $E_1$  is the equilibrium point corresponding to absence of cytokine and a low concentrations of the remaining components. Biologically, this case can be represented as when a relative small amount of LDL particles enters the arterial intima that will be converted into oxidized LDL, which are totally consumed by macrophages. In this case, we can note that the phagocytose process happens here without any significant effect from the inflammatory cytokines. Mathematically, this point can be stable or unstable.
- $E_2$  is the equilibrium point that can be classified as an intermediary unstable equilibrium whenever it exists. In other words, it can be illustrated as a threshold to overpass so that the display of an inflammation happens.
- $E_3$  is the equilibrium point that represents a large concentration of LDL, ox-LDL, immune cells and inflammatory cytokines simultaneously. This case can be classified as an inflammatory case biologically. Furthermore, we can not here that the relative high amount of inflammatory cytokines correlates with the display of an inflammatory reaction. Henceforth,  $E_3$  highlights the growing inflammation state and is invariably stable whenever it exists.

Subsequently, the proposed interpretation can be more conveniently given in terms of  $P$ , which represents to the permeability of the endothelium layer. We

can note here that the condition derived from stability of  $E_1$ :  $M^* < \frac{\lambda_2}{\alpha_2}$ , can be translated analytically into  $P < P^+ = \frac{1}{2L_0\alpha_L\beta_1\alpha_2^2}(\alpha_L\alpha_2\lambda_2L_0\alpha_M + \alpha_{Lox}\lambda_M\lambda_2^2 + \lambda_M\lambda_{Lox}\alpha_2\lambda_2 + \sqrt{(\alpha_L\alpha_2\lambda_2L_0\alpha_M)^2 + 4\alpha_L\beta_1\alpha_{Lox}\lambda_L\lambda_M L_0\lambda_2^2\alpha_2^2 + 4\alpha_L\beta_1\lambda_L L_0\lambda_M\lambda_{Lox}\lambda_2\alpha_2^3 + \kappa})$ , with  $\kappa = 2\alpha_L\alpha_{Lox}\alpha_2\lambda_M L_0\alpha_M\lambda_2^3 + 2\alpha_L\lambda_M\lambda_{Lox} L_0\alpha_M\alpha_2^2\lambda_2^2 + (\alpha_{Lox}\lambda_M)^2\lambda_2^4 + 2\alpha_{Lox}\alpha_2\lambda_{Lox}\lambda_M^2\lambda_2^3 + (\lambda_M\lambda_{Lox}\alpha_2\lambda_2)^2$ .

- If  $P = 0$ , No inflammatory reaction can set up.  $E_0$  is the only equilibrium point in this case.
- If  $P < P^-$ , indeed  $P$  is low, no inflammatory reaction can happen and the state stays in a disease free state. This is correlated with the existence of the unique fixed point  $E_1$  which is stable.
- If  $P^- < P < P^+$ , indeed  $P$  is considered as intermediary, we deduce two stable fixed points  $E_1$  and  $E_3$  and an unstable one  $E_2$ . This corresponds to the bistable case, where  $E_2$  will be considered as a threshold that the system has to overcome in order to pass from the non inflammatory state  $E_1$  to the inflammatory one  $E_3$ . Hence, the formation of an atherosclerotic plaque can happen if the initial perturbation is large enough to overcome the threshold, otherwise it will stay in the disease free state.
- If  $P > P^*$ , indeed  $P$  is large, there are two fixed points  $E_3$  being stable and  $E_1$  being unstable. This is classified as a monostable case where the only stable case is where we get high concentrations of all components. Hence, we can note here that a small perturbation of the non-inflammatory situation generates the launching of a chronic inflammatory reaction, which will lead to the development of a plaque.

The computation of  $P^-$  is provided in Appendix A.

# Chapter 4

## Existence and numerical simulations of travelling wave solutions

Recall the mathematical model:

$$\frac{\partial L}{\partial t} = d_L \frac{\partial^2 L}{\partial x^2} + P(L_0 - L) - \lambda_L L, \quad (4.1)$$

$$\frac{\partial Lox}{\partial t} = d_{Lox} \frac{\partial^2 Lox}{\partial x^2} + \alpha_L L - \alpha_{Lox} M Lox - \lambda_{Lox} Lox, \quad (4.2)$$

$$\frac{\partial M}{\partial t} = d_M \frac{\partial^2 M}{\partial x^2} + \frac{P(C + \beta_1 Lox)}{1 + \frac{C}{\tau_1}} - \alpha_M M Lox - \lambda_M M, \quad (4.3)$$

$$\frac{\partial C}{\partial t} = d_C \frac{\partial^2 C}{\partial x^2} + \frac{\alpha_2 M C}{1 + \frac{C}{\tau_2}} - \lambda_C C. \quad (4.4)$$

**Definition 4.0.1.** A travelling wave solution of system (4.1)-(4.4) is a particular solution that represents a propagating front with constant velocity  $c$ , connecting two equilibrium points of the kinetic system of system (4.1)-(4.4). It is expressed as:

$$\begin{pmatrix} L(t, x) \\ Lox(t, x) \\ M(t, x) \\ C(t, x) \end{pmatrix} = \omega(x - ct)$$

With  $c$  defined as a constant representing the speed of the wave and

$$\lim_{x \rightarrow \pm\infty} \omega(x) = \omega_{\pm} \quad (4.5)$$

with  $\omega_+$  and  $\omega_-$  being two equilibrium points of the kinetic system of system (4.1)-(4.4)

**Definition 4.0.2.** A system of partial differential equation is considered globally monotone, where the non diagonal components of its Jacobian matrix are non-negative.

In our case our initial Jacobian matrix is written as follows:

$$J = \begin{pmatrix} -P - \lambda_L & 0 & 0 & 0 \\ \alpha_L & -\alpha_{Lox}M - \lambda_{Lox} & -\alpha_{Lox}Lox & 0 \\ 0 & -\alpha_M M + \frac{P\beta_1}{1+\frac{C}{\tau_1}} & -\alpha_M Lox - \lambda_M & \frac{P - \frac{P\beta_1 Lox}{\tau_1}}{(1+\frac{C}{\tau_1})^2} \\ 0 & 0 & \frac{\alpha_2 C}{1+\frac{C}{\tau_2}} & \frac{\alpha_2 M}{(1+\frac{C}{\tau_2})^2} - \lambda_C \end{pmatrix}$$

The monotonicity of the proposed model fails because of the negative terms  $-\alpha_{Lox}Lox$ ,  $-\alpha_M M + \frac{P\beta_1}{1+\frac{C}{\tau_1}}$  and  $\frac{P - \frac{P\beta_1 Lox}{\tau_1}}{(1+\frac{C}{\tau_1})^2}$  in the Jacobian matrix. However, by imposing the following condition  $\beta_1 < 10^{-1}\tau_1$  along with checking that  $Lox$  is bounded, we solve the issue caused by the term  $P - \frac{P\beta_1 Lox}{\tau_1}$ , since the only source term in the equation of  $Lox$  is the oxidation of LDL ( $\alpha_L L$ ), which in return  $L$  is bounded by  $L_0 = 1.9$ , leading to say that  $Lox$  is as well bounded. Thus, the remaining two terms causing the non-monotonicity of our system are:  $-\alpha_{Lox}Lox$  and  $-\alpha_M M + \frac{P\beta_1}{1+\frac{C}{\tau_1}}$ . In order to solve the following issue we start by considering the term  $\alpha_{Lox} = \alpha_M = 0$  and try to find the equilibrium points of the reduced model along with their stability.

## 4.1 Updated Model with $\alpha_{Lox} = \alpha_M = 0$

In this part, we will study the following reduced kinetic model, which turns into :

$$\begin{cases} \frac{dL}{dt} = P(L_0 - L) - \lambda_L L, \\ \frac{dLox}{dt} = \alpha_L L - \lambda_{Lox} Lox, \\ \frac{dM}{dt} = \frac{P(C + \beta_1 Lox)}{1 + \frac{C}{\tau_1}} - \lambda_M M, \\ \frac{dC}{dt} = \frac{\alpha_2 M C}{1 + \frac{C}{\tau_2}} - \lambda_C C. \end{cases} \quad (4.6)$$

Looking at the equilibrium points of system (4.6), we have to distinguish between  $P = 0$  and  $P \neq 0$ :

### Case of zero permeability

If  $P = 0$ , the system (4.6) becomes:

$$\begin{cases} \lambda_L L = 0, \\ \alpha_L L - \lambda_{Lox} Lox = 0, \\ -\lambda_M M = 0, \\ \frac{\alpha_2 M C}{1 + \frac{C}{\tau_2}} - \lambda_C C = 0. \end{cases} \quad (4.7)$$

We get  $L^* = 0$ ,  $M^* = 0$ ,  $Lox^* = 0$  and  $C^* = 0$ . Then the fixed point in this case is  $E_0 = (L^*, Lox^*, M^*, C^*) = (0, 0, 0, 0)$

### Case of non-zero permeability

If  $P \neq 0$ , we get back the system (4.6):

$$\begin{cases} P(L_0 - L) - \lambda_L L = 0, \\ \alpha_L L - \lambda_{Lox} Lox = 0, \\ \frac{P(C + \beta_1 Lox)}{1 + \frac{C}{\tau_1}} - \lambda_M M = 0, \\ \frac{\alpha_2 M C}{1 + \frac{C}{\tau_2}} - \lambda_C C = 0. \end{cases} \quad (4.8)$$

After solving the first equation we get  $L^* = \frac{PL_0}{P + \lambda_L}$ .

The fourth equation of (4.6) leads to either  $C = 0$  or  $M = \frac{\lambda_C}{\alpha_2} \left(1 + \frac{C}{\tau_2}\right)$ .

**Nullclines on the hyperplane  $C=0$ .** For  $C = 0$  and  $L^* = \frac{PL_0}{P + \lambda_L}$ , we can directly get  $Lox^* = \frac{\alpha_L}{\lambda_{Lox}} L^*$ . Also, by solving the fourth equation we get  $M^* = \frac{P\beta_1 Lox^*}{\lambda_M}$ . Thus we get one fixed point  $E_1 = (L^*, Lox^*, M^*, 0)$ .

**Nullclines on the hyperplane  $M = \frac{\lambda_C}{\alpha_2} \left(1 + \frac{C}{\tau_2}\right)$ .** Similarly in this case we

have  $L^* = \frac{PL_0}{P + \lambda_L}$ ,  $Lox^* = \frac{\alpha_L}{\lambda_{Lox}} L^*$ . Working on the remaining two last equations,

we get: 
$$\begin{cases} M = g_1(C) := \frac{\lambda_C}{\alpha_2} \left(1 + \frac{C}{\tau_2}\right), \\ M = g_2(C) := \frac{P(C + \beta_1 Lox^*)}{\lambda_M \left(1 + \frac{C}{\tau_1}\right)}. \end{cases}$$

By equating  $g_1 = g_2$ , we get:

$$\frac{\lambda_C}{P\beta_1Lox^*\tau_1\tau_2}C^2 + \left(\frac{\lambda_C}{\alpha_2}\left(\frac{1}{\tau_1} + \frac{1}{\tau_2}\right) - \frac{P}{\lambda_M}\right)C + \left(\frac{\lambda_C}{\alpha_2} - \frac{P\beta_1Lox^*}{\lambda_M}\right) = 0 \quad (4.9)$$

Hence we can deduce three possible cases for the intersection between the line  $g_1$  and the curve  $g_2$ :

- If  $\frac{\lambda_C}{\alpha_2} < \frac{P\beta_1Lox^*}{\lambda_M}$ , Only one non-negative solution of equation (4.5) exist, denoted by  $C_3$ . Then. denote by  $E_3 = (L^*, Lox^*, M_3, C_3)$  the corresponding equilibrium point.
- Let  $\frac{P\beta_1Lox^*}{\lambda_M} < \frac{\lambda_C}{\alpha_2} < \frac{P\tau_1}{\lambda_1}$ 
  - If  $0 < \frac{\lambda_C}{\alpha_2\tau_2} < \left(\sqrt{\frac{P}{\lambda_M} - \frac{P\beta_1Lox^*}{\tau_1\lambda_M}} - \sqrt{\frac{\lambda_C}{\alpha_2\tau_1} - \frac{P\beta_1Lox^*}{\tau_1\lambda_M}}\right)^2$ , then there exists two non-negative solutions of equations (4.5) denoted by  $E_2$  and  $E_3$  with  $E_2 = (L^*, Lox^*, M_2, C_2)$  and  $E_3 = (L^*, Lox^*, M_3, C_3)$ .
  - If  $\left(\sqrt{\frac{P}{\lambda_M} - \frac{P\beta_1Lox^*}{\tau_1\lambda_M}} - \sqrt{\frac{\lambda_C}{\alpha_2\tau_1} - \frac{P\beta_1Lox^*}{\tau_1\lambda_M}}\right)^2 < \frac{\lambda_C}{\alpha_2\tau_2}$ , then there is no positive solution to equation (4.5).
- If  $\frac{P\tau_1}{M} < \frac{\lambda_C}{\alpha_2}$ , equation (4.9) admits no positive solutions.

#### 4.1.1 Equilibrium Points' Stability

In this part, we study the stability of the equilibrium points  $E_0, E_1, E_2$  and  $E_3$  when they exist. Mathematically, stability of a fixed point can be found analytically by finding the real part sign of the eigenvalues of the Jacobian matrix.

The Jacobian matrix in this case is as following :

$$J = \begin{pmatrix} -P - \lambda_L & 0 & 0 & 0 \\ \alpha_L & -\lambda_{Lox} & 0 & 0 \\ 0 & \frac{P\beta_1}{1+\frac{C}{\tau_1}} & -\lambda_M & \frac{P - \frac{P\beta_1Lox}{\tau_1}}{\left(1+\frac{C}{\tau_1}\right)^2} \\ 0 & 0 & \frac{\alpha_2 C}{1+\frac{C}{\tau_2}} & \frac{\alpha_2 M}{\left(1+\frac{C}{\tau_2}\right)^2} - \lambda_C \end{pmatrix}$$

Clearly, in this case, we can notice the off-diagonal elements of the Jacobian matrix are positive.

**Stability of  $E_0$ .** We can replace in  $J$  the values of  $E_0$ , we get that all eigenvalues are negative, leading to  $E_0$  being stable.

**Stability of  $E_1$ .** In a similar manner, we can replace by the values of  $E_1$  in the  $J$  and find that 3 out of 4 eigenvalues are negative and the fourth one has a negative real part if  $M^* = \frac{P\beta_1 L\alpha x^*}{\lambda_M} < \frac{\lambda_C}{\alpha_2}$ . Consequently we can derive that  $E_1$  is stable or unstable.

**Stability of  $E_2$ .** Using a Trace-Determinant analysis along with the following graphical properties:  $g_2$  is concave and  $g_1$  a straight line, we get that  $E_2$  is unstable.

**Stability of  $E_3$ .** In a similar manner as for  $E_2$ , we get that  $E_3$  is a stable equilibrium.

## 4.2 Complete model

In this part, we study existence and stability of solutions for system (4.1)-(4.4), with  $\alpha_{Lox}$  and  $\alpha_M$  are both positive. In order to follow with this work, we will be implementing the implicit function theorem.

**Theorem 4.2.1.** *Let  $B_1$  and  $B_2$  be two Banach spaces and  $(\epsilon, Q) \in B_1 \times B_2$ . Let  $x \in [0, 1]$  and  $Q(x)$  be a  $C^2([0, 1])$  class function with  $Q(0) = 0$  and  $Q(1) = 0$ . Define  $G$  to be a function such that  $G(Q)$  is a  $C^1$  function with  $G(E) = 0$ . Define  $b$  to be a constant. Suppose that in a neighborhood  $D$  of a point  $(0, E) \in B_1 \times B_2$ , we define an operator  $A(\epsilon, Q) = bQ'' + G(Q) + \epsilon f(x)$ , that maps into  $F$ , a Banach space.*

*When  $G'(E) \neq k^2\pi^2, \forall k \in \mathbb{N}$ , we prove existence of an operator  $\Phi$  defined in some neighborhood  $N \subset B_1$  of the point 0. This operator maps its respective neighborhood into the Banach space  $B_2$ . In addition, the operator  $\Phi$  is uniquely determined by the subsequent properties:*

- $A(\epsilon, \Phi(\epsilon)) = 0$ .
- $\Phi(0) = E$ .
- $\Phi$  admits continuity at 0.

*With respect to all theorem's condition, if continuity of  $A$  is proved everywhere in  $D$ , thus the continuity of the operator  $\Phi$  in some neighborhood of the point 0 is also proved. Furthermore, if the existence of the partial derivative  $A'_\epsilon$  in  $D$  and its continuity at  $(0, E)$  are assumed, therefore the derivative of the operator  $\Phi$  exists at 0 and*

$$\Phi'(0) = -(A'_Q(0, E))^{-1}A'_\epsilon(0, E) \quad (4.10)$$

*Proof.* Note that we can use the following:

$$A'_Q(\epsilon, Q)V = \left[ \frac{d}{dt} A(\epsilon, Q + tV) \right]_{t=0} = bV'' + VG'(Q). \quad (4.11)$$

We consider the following particular case:

$$\left[ \frac{d}{dt} A(\epsilon, Q + tV) \right]_{Q=E, t=0} = bV'' + VG'(E) \quad (4.12)$$

Define the operator  $L: C^2([0, 1]) \rightarrow C^0([0, 1])$ , such that  $\forall V \in C^2([0, 1])$ ,  $LV = bV'' + G'(E)V$ .

Also,  $A(\epsilon, Q)$  about  $Q = E$  can be approximated by the expression of  $LV$ .

After the substitution,  $V(0) = 0$  and  $V(1) = 0$  become the boundary conditions.

Then, we have :

- $A$  is continuous on  $D$  that includes  $(0, E)$  and  $A(0, E) = 0$ .
- Since  $G$  is of class  $C^1$ , the operator  $A'_Q$  defined as  $A'_Q(\epsilon, Q) = b \frac{d^2}{dx^2} + G'(Q)$  exists.

Then, the continuity of  $A'_Q$  at  $(0, E)$  can be checked:

Starting with the continuity of  $G'$ , there exists  $R_0$ , such that  $\forall \kappa > 0$ , if  $\|Q - E\|_{C^2} < R_0$ , then  $\|G'(Q) - G'(E)\| < \kappa$ .

Let  $(\epsilon, Q)$  be near  $(0, 0)$ , there exist  $D_1$  and  $D_2$ , such that  $|\epsilon| < D_1$  and  $\|Q - E\|_{C^2} < \min(R_0, D_2)$ .

$$\begin{aligned} \|A'_Q(\epsilon, Q) - A'_Q(0, E)\| &= \sup_{\|V\| \leq 1} \|A'_Q(\epsilon, Q - A'_Q(0, E))V\| \\ &= \sup_{\|V\| \leq 1} \|G'(Q)V - G'(E)V\| \\ &\leq \|G'(Q) - G'(E)\| \sup_{\|V\| \leq 1} \|V\| \\ &= \|G'(Q) - G'(E)\| \\ &\leq \kappa \forall \kappa > 0. \end{aligned}$$

- $A'_Q(0, E) = L$  is an operator from  $B_2$  into  $F$ . In order to get the spectrum of the operator  $L$ , denote by  $\lambda$  an eigenvalue of  $L$ . Then for  $V \in C^2([0, 1])$ ,  $LV = \lambda V$  provides:

$$bV'' + (G'(E) - \lambda)V = 0 \quad (4.13)$$

Therefore,  $\lambda = G'(E) - k^2\pi^2$  for  $k \in \mathbb{N}$ . The expression  $G'(E)$  is a constant or generally  $|G'(E) - \lambda I| = 0$ .

Then, we can deduce the following: If  $G'(E) \neq k^2\pi^2, \forall k \in \mathbb{N}$  (indeed, the

Jacobian matrix at  $E$  has non-zero eigenvalues), then the operator  $L$  has an inverse.

Note that the operator  $L$  is bounded because the given linear operator is continuous between two normed spaces.

In addition, since the operator  $L$  is bounded and has an inverse, we get that its respective inverse is also bounded. Here, we have used the bounded inverse theorem that states : A bijection bounded linear operator, that maps a Banach space into another one, has a bounded inverse.

Finally, one can state that applying the implicit function theorem to  $A(\epsilon, Q)$  if  $G'(E) \neq k^2\pi^2$ , can be done  $\forall k \in \mathbb{N}$ .

**Corollary 4.2.1.** *Define the following polynomial of the form  $p(x, y) = y^n + a_{n-1}(x)y^{n-1} + \dots + a_1(x)y + a_0(x)$  with coefficients that depend smoothly on a parameter  $x$ . If for  $x = 0$ , the value  $y = y_0$  represents a simple root of the polynomial  $p(0, y_0) = 0$ , then for all  $x$  sufficiently close to 0, we can prove existence of a unique root  $y(x)$  with  $y(0) = y_0$  that smoothly depends on  $x$ .*

*Proof.* Having  $p(0, y_0) = 0$ , we keen to solve  $p(x, y) = 0$  for  $y(x)$  with  $y(0) = y_0$ . The followed affirmation is directly proven because of the implicit function theorem.  $p(0, y)$  can be written as  $p(0, y) = (y - y_0)g(y)$  due to  $y(0) = y_0$  being a simple root of  $p(0, y) = 0$ , with  $g(y_0) \neq 0$ . Therefore, the derivative  $p_y(0, y_0) \neq 0$ .

**Theorem 4.2.2.** *Given a square matrix  $A(x)$  whose elements depend smoothly on a real parameter  $x$ , if  $\lambda = \lambda_0$  is a simple eigenvalue at  $x = 0$ , then for all  $x$  near 0 there is a respective eigenvalue that also depends smoothly on the same parameter  $x$ .*

*Proof.* By applying Corollary 4.2.1 to the characteristic polynomial of the matrix  $A(x)$ , we get a direct and immediate proof.

### 4.2.1 Perturbed Solution with $\alpha_M > 0$ and $\alpha_{Lox} = 0$

First, we fix  $\alpha_{Lox} = 0$  and consider  $\alpha_M > 0$  in equations (2.1)-(2.4). Second, we check existence of an analytical solution near

$E_1 = (L^* = \frac{PL_0}{P+\lambda_L}, Lox^* = \frac{\alpha_L}{\lambda_{Lox}}L^*, M^* = \frac{P\beta_1Lox^*}{\lambda_M}, 0)$  when  $\alpha_M$  is located in a sufficiently tiny neighborhood of 0 then we elaborate on its stability. We can get the similar results for  $E_3$  by following a similar procedure.

Denote by  $A$  the operator :  $A(\alpha_M, Q) : B(0, 1) \times C^2([0, 1]) \rightarrow C^0([0, 1])$  be defined in a neighborhood  $D$  of the point  $(0, E_1) \in B(0, 1) \times C^2([0, 1])$ , in such a way  $A(\alpha_M, Q) = F(Q) + \alpha_M f(x)$ , where :

$$Q = \begin{pmatrix} L \\ Lox \\ M \\ C \end{pmatrix}, F(Q) = \begin{pmatrix} P(L_0 - L) - \lambda_L L \\ \alpha_L L - \lambda_{Lox} Lox \\ \frac{P(C + \beta_1 Lox)}{1 + \frac{C}{\tau_1}} - \lambda_M M \\ \frac{\alpha_2 M C}{1 + \frac{C}{\tau_2}} - \lambda_C C \end{pmatrix} \text{ and } f(x) = \begin{pmatrix} 0 \\ 0 \\ -M Lox \\ 0 \end{pmatrix}$$

Assuming that  $Q(x)$  is non negative-values  $C^2([0, 1])$  functions in such a way:  $Q(0) = 0$  and  $Q(1) = 0$ .

$F(Q)$  is a function of class  $C^1$  with  $F(E_1) = 0$ .

Note here that  $A(0, E_1) = 0$ . Furthermore, eigenvalues of the Jacobian matrix of system (2.1)-(2.4) at  $E_1$  are  $-P - \lambda_L$ ,  $-\lambda_{Lox}$ ,  $-\lambda_M$  and  $\alpha_2 M - \lambda_C$ , and none of the four eigenvalues is zero.

Hence, an operator  $\Phi$  exists and is defined in a neighborhood  $W \subset B(0, 1)$  of the point 0.  $\Phi$  maps  $W$  into the space  $C^2([0, 1])$  and contents the below three properties :

- $A(\alpha_M, \Phi(\alpha_M)) = 0$  in  $G$ .
- $\Phi(0) = E_1$ .
- $\Phi$  is continuous at 0.

Now, we can denote  $F_1 = \Phi(E_1)$ . Especially, when  $\alpha_M \in W$  and  $\alpha_M > 0$ . the system admits a solution  $F_1$  near  $E_1$  in the positive half space.

The next step will consist of checking the stability of  $F_1$ . Then we look at the Jacobian matrix of the kinetic system (2.1)-(2.4) with  $\alpha_{Lox} = 0$  at  $F_1$ . Since the Jacobian is a square 4 by 4 matrix whose elements smoothly depend on  $\alpha_M$ . Implementing Theorem 4.2.2, if  $\lambda_0$  is a simple eigenvalue at  $E_1$ , then for all  $t$  near 0 there is a respective eigenvalue that depends smoothly on the parameter  $\alpha_M$ . Hence, since all eigenvalues of the Jacobian matrix defined at  $E_1$  are simple roots, with  $\alpha_M$  taken to be small enough, each eigenvalue of the Jacobian matrix at  $F_1$  lies in a small neighborhood whose center is the respective eigenvalue of the Jacobian matrix at  $E_1$ . To sum it up, we can state that the Jacobian's eigenvalues at  $F_1$  are all simple and real and have similar sign as the eigenvalues at  $E_1$ . Therefore, we deduct that when  $E_1$  is stable and  $\alpha_M$  close enough to 0, we get  $F_1$  is stable.

#### 4.2.2 Perturbed Solution with $\alpha_M > 0$ and $\alpha_{Lox} > 0$

Following a similar manner as in subsection 4.2.1, proving that the system (4.1)-(4.4) has two equilibrium points  $W_1$  and  $W_3$  with  $\alpha_M > 0$  and  $\alpha_{Lox} > 0$ , we take into consideration  $A^*(\alpha_{Lox}, Q) : B(0, 1) \times C^2([0, 1]) \rightarrow C^0([0, 1])$  to be given in

$D$  a neighborhood of the point  $(0, F_1) \in B(0, 1) \times C^2([0, 1])$  in such a way that  $A^*(\alpha_{Lox}, Q) = F(Q) + \alpha_{Lox}f^*(x)$ , with:

$$Q = \begin{pmatrix} L \\ Lox \\ M \\ C \end{pmatrix}, F(Q) = \begin{pmatrix} P(L_0 - L) - \lambda_L L \\ \alpha_L L - \lambda_{Lox} Lox \\ \frac{P(C + \beta_1 Lox)}{1 + \frac{C}{\tau_1}} - \alpha_M M Lox - \lambda_M M \\ \frac{\alpha_2 M C}{1 + \frac{C}{\tau_2}} - \lambda_C C \end{pmatrix} f^*(x) = \begin{pmatrix} 0 \\ -M Lox \\ 0 \\ 0 \end{pmatrix}$$

We proceed in the same manner as above, and we can conclude as well that  $W_1$  and  $W_3$  are stable respectively when  $E_1$  and  $E_3$  are stable.

To sum everything up, this chapter is concerned on proving the existence of travelling wave solution for system (4.1)-(4.4). Hence, the implicit function theorem was applied to the updated monotone model (4.6). We start by considering the updated model for  $\alpha_{Lox} = 0$  and  $\alpha_M$  begin sufficiently small. Then, a proof on the existence of two equilibrium point  $F_1$  and  $F_3$  near  $E_1$  and  $E_3$  respectively. The proof is completed by showing the stability analysis for  $F_1$  and  $F_3$  that correspond to the stability of  $E_1$  and  $E_3$  respectively. Subsequently, we take into account that  $\alpha_{Lox} > 0$  and  $\alpha_M > 0$  being both sufficiently small, a similar procedure as above is used to prove existence and show stability of the two equilibrium points  $W_1$  and  $W_3$  near  $F_1$  and  $F_3$ .

### 4.3 Numerical results

In order to present previous results using numerical simulation, we get back to solving the system (2.1)-(2.4) on the one dimensional interval  $x \in ]0, 1[$  with homogeneous Neumann boundary conditions. All diffusion terms will be considered  $10^{-3}$  and remaining parameters values will be taken as of Table (2.1), by taking into account the imposed conditions from sections 4.1 and 4.2 derived from the Implicit function theorem. We will be considering the parameter of the permeability  $P$  as variable, by taking the following case:

- Case 1: Zero Permeability  $P = 0$

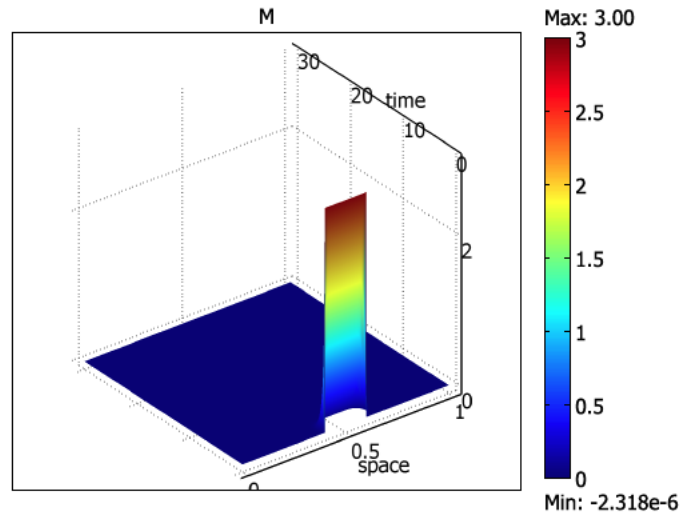


Figure 4.1: In case 1, a large perturbation of the the non-inflammatory state does not conduct to the propagation of a chronic inflammatory reaction.

- Case 2: Low Permeability

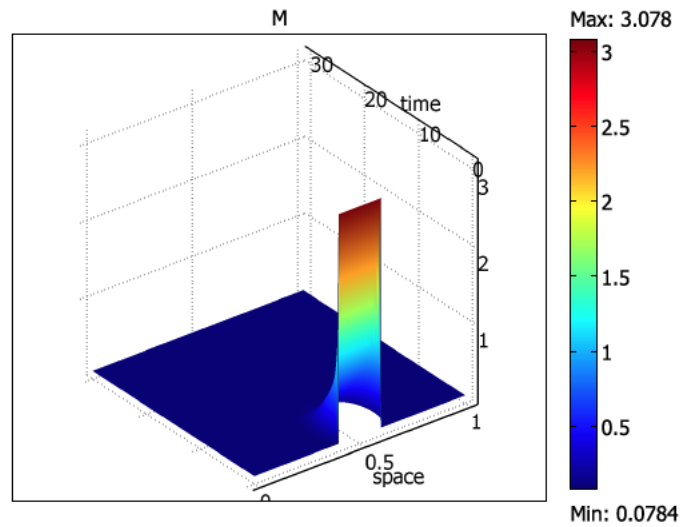


Figure 4.2: In case 2, a large perturbation of the the non-inflammatory state does not lead to the propagation of a chronic inflammatory reaction.

- Case 3: Intermediate Permeability
  - Case 3.1: Initial condition being a small perturbation

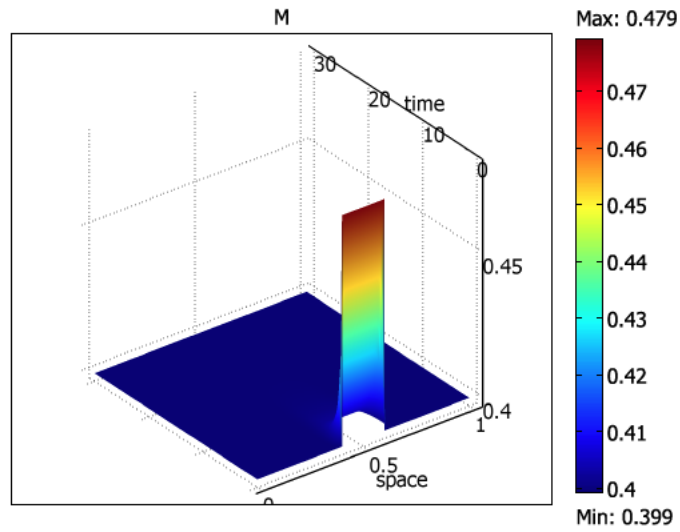


Figure 4.3: In case 3.1, a small perturbation of the non-inflammatory state does not lead to the propagation of a chronic inflammatory reaction.

- Case 3.2: Initial condition being a large perturbation

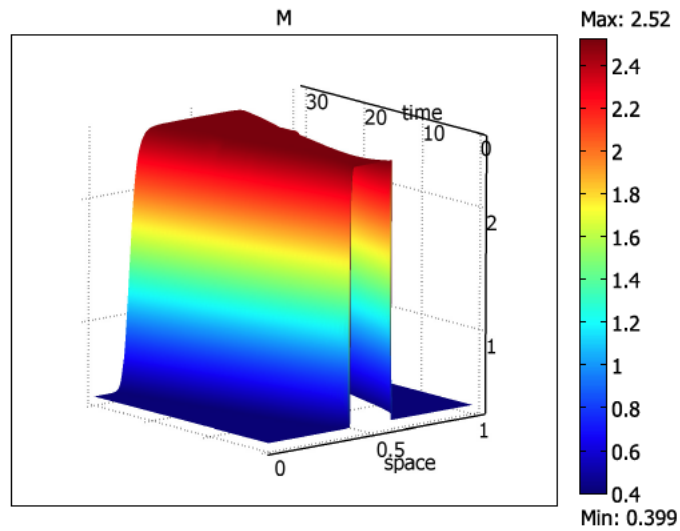


Figure 4.4: In case 3.2, a large perturbation of the non-inflammatory state leads to a wave propagation that corresponds to a chronic inflammatory reaction.

- Case 4: High permeability

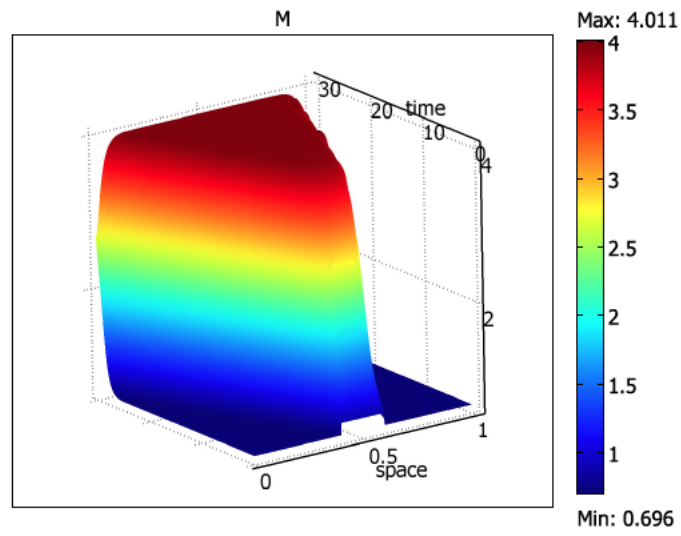


Figure 4.5: In case 4, even a small perturbation of the non-inflammatory state leads to a wave propagation that corresponds to a chronic inflammatory reaction.

# Chapter 5

## Discussion

Atherosclerosis is generally considered an inflammatory disease that is usually modeled using partial differential equations. In this thesis, we have considered a coupled system of four partial differential equations of diffusion-reaction type in order to model one of the first stages of atherosclerosis that is the inflammatory stage. The four main leading players are the concentrations of low density lipoproteins (LDL), cytokines, oxidized low density lipoproteins (ox-LDL) and immune cells (monocytes and macrophages). Moreover, the role and effect of the permeability of the endothelial layer on the arise of an inflammatory reaction in the arterial intima is highlighted and taken into account in this model. Also, this study presented the atherosclerotic inflammation as a travelling wave that propagates in the interior of the arterial intima. The proof of existence of travelling wave solution is performed in two ways. Both ways, analytical and numerical, conducted to provide a categorization of the various states of the disease with respect to the permeability of the endothelium layer.

It is generally agreed that the atherosclerotic process involve various biochemical and mechanical phenomena that are considered complicated along with a large numbers of risk factors that assist this process [20]. This work is considered to be biologically and mathematically challenging because of the presence of four agents along with the permeability of the endothelium wall. We are able to distinguish three main cases of the disease state that correlates with the permeability of the endothelial layer; where we can note that the permeability is classified according to its value based on the remaining parameters. In fact, when the permeability is low, this case is considered to be the disease free state since no chronic inflammatory reaction occurs due to the non initiation of the auto-amplification process. With intermediate permeability, if the system overcomes a threshold, a perturbation of the non-inflammatory state might conduct to a wave propagation corresponding to a chronic inflammatory reaction. Else, the system turns back to the non-inflammatory state. With high permeability, even a small perturbation

of the disease free situation drives to a wave propagation representing a chronic inflammatory reaction.

This research work can be further expanded by considering a possible expansion to a 2D model where the geometry represents the arterial intima. For instance, in [10] an expansion from the 1D to the 2D model is done and the recruitment of immune cells appears to be a boundary condition. Moreover, another further enhancement can be adding additional key players to the model such as HDL (high density lipoproteins), free radicals, inhibitors of the inflammation and foam cells. In other words, by increasing the number of lead players as well as the number of parameters, we expect a more realistic representation of the atherosclerotic process.

Further development of the model can be the representation of the permeability of the endothelium layer in function of the risk factors. In fact, many risk factors such as hypertension and smoking might be taken into account. In addition, other disrupters of the endothelium permeability such as shear stress, nitric oxide concentration and endothelium glycocalyx can be as well taken into account. Henceforth, the action of permeability can be better illustrated not only in function of values but in term of biological essence.

# Bibliography

- [1] Hannah Ritchie and Max Roser. *Causes of Death*. Our World In Data, 2018, <https://ourworldindata.org/causes-of-death>.
- [2] GBD 2019 Diseases and Injuries Collaborators (2020). *Global burden of 369 diseases and injuries in 204 countries and territories, 1990-2019: a systematic analysis for the Global Burden of Disease Study 2019*. *Lancet* (London, England), 396(10258), 1204–1222. [https://doi.org/10.1016/S0140-6736\(20\)30925-9](https://doi.org/10.1016/S0140-6736(20)30925-9)
- [3] Mc Namara, K., Alzubaidi, H., Jackson, J. K.. *Cardiovascular disease as a leading cause of death: how are pharmacists getting involved?* *Integrated pharmacy research practice*, 8, 1–11. <https://doi.org/10.2147/IPRP.S133088> (2019)
- [4] Cobbold, C.A., Sherratt, J.A. Maxwell, S.R.J. *Lipoprotein oxidation and its significance for atherosclerosis: A mathematical approach*. *Bull. Math. Biol.* 64, 65–95 (2002). <https://doi.org/10.1006/bulm.2001.0267>
- [5] Evans, P. C., Rainger, G. E., Mason, J. C., Guzik, T. J., Osto, E., Stamataki, Z., Neil, D., Hofer, I. E., Fragiadaki, M., Waltenberger, J., Weber, C., Bochaton-Piallat, M. L., Bäck, M. (2020). *Endothelial dysfunction in COVID-19: a position paper of the ESC Working Group for Atherosclerosis and Vascular Biology, and the ESC Council of Basic Cardiovascular Science*. *Cardiovascular research*, 116(14), 2177–2184. <https://doi.org/10.1093/cvr/cvaa230>
- [6] Davignon, J., Ganz, P. (2004). *Role of endothelial dysfunction in atherosclerosis*. *Circulation*, 109(23 Suppl 1), III27–III32. <https://doi.org/10.1161/01.CIR.0000131515.03336.f8>
- [7] Yilmaz, O., Afsar, B., Ortiz, A., Kanbay, M. (2019). *The role of endothelial glycocalyx in health and disease*. *Clinical kidney journal*, 12(5), 611–619. <https://doi.org/10.1093/ckj/sfz042>

- [8] Mundi, S., Massaro, M., Scoditti, E., Carluccio, M. A., van Hinsbergh, V., Iruela-Arispe, M. L., De Caterina, R. (2018). *Endothelial permeability, LDL deposition, and cardiovascular risk factors-a review*. Cardiovascular research, 114(1), 35–52. <https://doi.org/10.1093/cvr/cvx226>
- [9] Mannarino, E., Pirro, M. (2008). *Molecular biology of atherosclerosis*. Clinical cases in mineral and bone metabolism : the official journal of the Italian Society of Osteoporosis, Mineral Metabolism, and Skeletal Diseases, 5(1), 57–62.
- [10] N. El Khatib, S. Génieys, B. Kazmierczak, V. Volpert. *Mathematical modelling of atherosclerosis as an inflammatory disease*. Math. Model. Nat. Phenom. Vol. 2, No. 2, 2007, 126-141 .
- [11] Abi Younes G, El Khatib N. *Mathematical modeling of atherogenesis: Atheroprotective role of HDL*. Journal of Theoretical Biology. 2021 Nov 21;529:110855. doi: 10.1016/j.jtbi.2021.110855.
- [12] Libby P. (2021). *The changing landscape of atherosclerosis*. Nature, 592(7855), 524–533. <https://doi.org/10.1038/s41586-021-03392-8>
- [13] Formaggia, Luca Quarteroni, Alfio Veneziani, Alessandro. (2009). *Mathematics: Modeling and Simulation of the Circulatory System*. 10.1007/978-88-470-1152-6.
- [14] Karimi, S., Dadvar, M., Modarress, H., Dabir, B. (2013). *Kinetic modeling of low density lipoprotein oxidation in arterial wall and its application in atherosclerotic lesions prediction* . Chemistry and physics of lipids, 175-176, 1–8. <https://doi.org/10.1016/j.chemphyslip.2013.07.006>
- [15] N. El Khatib, S. Génieys, B.Kazmierczak, V. Volpert.*Reaction-diffusion model of atherosclerosis development* . J Math Biol. Vol. 65, No. 2, 2012, 349- 74.
- [16] Hao, W., Friedman, A. (2014). *The LDL-HDL profile determines the risk of atherosclerosis: a mathematical model*. PloS one, 9(3), e90497. <https://doi.org/10.1371/journal.pone.0090497>
- [17] G. Abi Younes, N. El Khatib. *Mathematical modeling of inflammatory processes of atherosclerosis* Math. Model. Nat. Phenom. 17 5 (2022). DOI: 10.1051/mmnp/2022004

- [18] Telma Silva, Willi Jäger, Maria Neuss-Radu, Adélia Sequeira, *Modeling of the early stage of atherosclerosis with emphasis on the regulation of the endothelial permeability*, Journal of Theoretical Biology, Volume 496, 2020, 110229, ISSN 0022-5193, <https://doi.org/10.1016/j.jtbi.2020.110229>.
- [19] Cameron McKay, Sean McKee, Nigel Mottram, Tony Mulholland and Stephen Wilson. *Towards a Model of Atherosclerosis*. Research report, University of Strathclyde (2004)
- [20] Fan, J., Watanabe, T. (2003). Inflammatory reactions in the pathogenesis of atherosclerosis. *Journal of atherosclerosis and thrombosis*, 10(2), 63–71. <https://doi.org/10.5551/jat.10.63>

# Appendices

# Appendix A

## Computations

### A.0.1 Detailed computation for the case presented in (2.2.2)

Finding the equilibrium points on the plane  $M = \frac{\lambda_C}{\alpha_2}(1 + \frac{C}{\tau_2})$  lead to solve the following system of equation :

$$\begin{cases} M=g_1(C) := \frac{(PC\alpha_{Lox}-\alpha_M\alpha_L L^*(1+\frac{C}{\tau_1})-\lambda_M\lambda_{Lox}(1+\frac{C}{\tau_1}))+\sqrt{\Delta}}{2\lambda_M\alpha_{Lox}(1+\frac{C}{\tau_1})}, \\ M=g_2(C) := \frac{\lambda_C}{\alpha_2}(1 + \frac{C}{\tau_2}) \end{cases} \quad (A.1)$$

By equating  $g_1(C) = g_2(C)$ , we get:

$$\frac{1}{\alpha_2^2\tau_1^2\tau_2^2} (4\alpha_{Lox}\lambda_M(\tau_1 + C)(C^3 + AC^2 + BC + D)) = 0 \quad (A.2)$$

where  $A = \frac{-L^*\alpha_L\tau_2\alpha_2\lambda_C\alpha_M + \alpha_{Lox}\alpha_2\lambda_C P\tau_1\tau_2 - \alpha_{Lox}\lambda_M\lambda_C^2\tau_1 - 2\alpha_{Lox}\lambda_M\lambda_C^2\tau_2 - \lambda_M\lambda_{Lox}\lambda_C\alpha_2}{-\alpha_{Lox}\lambda_M\lambda_C^2}$ ,  
 $B = \frac{-L^*\alpha_L\alpha_2\tau_1\tau_2\alpha_M - L^*\alpha_L\alpha_2\lambda_C\tau_2^2\alpha_M + \alpha_{Lox}\alpha_2\lambda_C P\tau_1\tau_2^2 + \lambda_{Lox}\alpha_2^2 P\tau_1\tau_2^2 - 2\alpha_{Lox}\lambda_M\lambda_C^2\tau_1\tau_2\Gamma}{-\alpha_{Lox}\lambda_M\lambda_C^2}$ ,  
 $D = \frac{L^*\alpha_L\beta_1\alpha_2^2 P\tau_1\tau_2^2 - L^*\alpha_L\alpha_2\lambda_C\tau_1\tau_2^2\alpha_M - \alpha_{Lox}\lambda_M\lambda_C^2\tau_1\tau_2^2 - \lambda_M\lambda_{Lox}\alpha_2\lambda_C\tau_1\tau_2^2}{-\alpha_{Lox}\lambda_M\lambda_C^2}$ ,  $L^* = \frac{PL_0}{P+\lambda_L}$  and  
 $\Gamma = -\alpha_{Lox}\lambda_M\lambda_C^2\tau_2^2 - \lambda_M\lambda_{Lox}\alpha_2\lambda_C\tau_1\tau_2 - \lambda_M\lambda_{Lox}\alpha_2\lambda_1\tau_2^2$

We get that  $C_1 = -\tau_1 < 0$ , which is not taken into consideration. Hence, it remains to solve the 3rd order degree polynomial in  $C$ , we seek in that case where we have existence of 3 real roots. Mathematically, it means that the roots of the derivative of  $f(C) = C^3 + AC^2 + BC + D$ , are real, and their image product with respect to  $f$  is negative, leading to the following two conditions to be satisfies in order to have the existence of two intersection points in the positive plane

$$\text{between } g_1 \text{ and } g_2: \begin{cases} 4A^2 - 12B > 0, \\ 4DA^2 - B^2A^2 - 18ABD + 4B^3 + 27D^2 < 0 \end{cases}$$

Note here, that if the two conditions are satisfied, we get the existence of one equilibrium point who is always located in the positive plane denoted by  $E_3$ . In addition, when the two conditions are satisfied along with the condition derived

in Chapter 3, that is  $P < P^+$ , we get the existence of the second equilibrium point in the positive plane denoted by  $E_2$ .

Both conditions obtained can be as well translated in function of the key parameter  $P$ , leading to an additional constant parameter  $P^-$  in function of all the constant parameters.

**Numerical existence of  $P^-$ .** Here, we consider the two conditions translated in function of the key parameter  $P$ , where all remaining parameters are taken as in Table (2.1), such that the colored regions are where the conditions are satisfied with respect to  $P$ .

- Condition 1:  $4A^2 - 12B > 0$

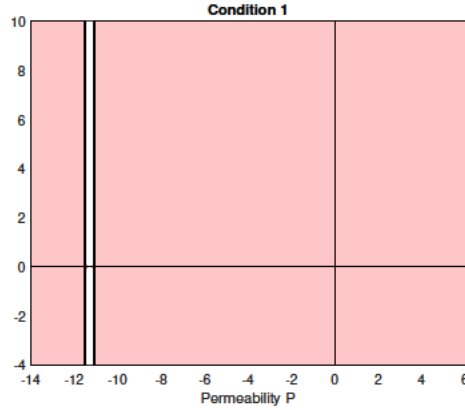


Figure A.1: Translation of condition 1 as function of  $P$ .

- Condition 2:  $4DA^2 - B^2A^2 - 18ABD + 4B^3 + 27D^2 < 0$

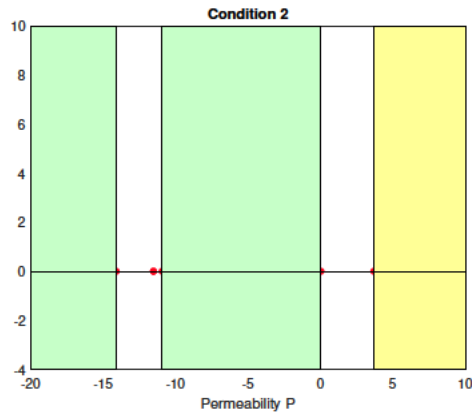


Figure A.2: Translation of condition 2 as function of  $P$ .

Condition 1 is always satisfied in our case, since we are only considering where the permeability value is positive. However, condition 2 is satisfied for positive values of  $P$  for  $0 < P < 0.0328$  and  $P > 3.678$ . But, for  $0 < P < 0.0328$ ,

the two intersection between  $g_1$  and  $g_2$  is in the negative half plane, then this case will not be taken into consideration. In opposition for  $P > 3.678$ , where we get existence of two equilibrium points denoted by  $E_2$  and  $E_3$ . Furthermore, for results checking procedure, we can check figure 2.6, where a bifurcation diagram is presented showing the concentration of immune cells of the stable equilibrium points in function of  $P$ . In fact, the value of  $P^- = 3.678$  exists and is the threshold to overpass between the existence of one and two stable equilibrium points. Moreover, the value of  $P^+ = 6.35$ , whose analytical expression is given in Chapter 3, is also well highlighted to be the threshold between the existence of two and one equilibrium points.

# Appendix B

## Matlab Codes

```
1 function plotequilibriumpoints
2 % This function plots the equilibrium points in all 3 cases, using the
3 % intersection of functions g1 and g2
4 lo=1.90;%L0
5 d=12.096;%LambdaL
6 a=d; %alphaL
7 b=0.05; %beta1
8 w=0.0120096; %alphaM
9 c=0.01; %alphaLox
10 g=2.0736; %LambdaLox
11 m=1.188; %Lambda2
12 j=2;%alpha2
13 t=1.4;%tau1
14 v=42/43;%tau2
15 f=1.9872;%LambdaM
16
17 syms x;
18 %p=1; %% Low Permeability
19 %p=5; %%Intermediate Permeability
20 %p=7; %%High Permeability
21
22 L=p*lo/(p+d); %Get L*
23 g1(x)=m*(1+x./v)./j;
24 g2(x)=((p*x*c-w*a*L*(1+x./t)-f*g*(1+x./t)) );
25 re=4*f*c*(1+x./t)*(p*x*g+p*a*L*b);
26 g2(x)=g2(x)+sqrt((p*x*c-w*a*L*(1+x./t)-f*g*(1+x./t))^2+re);
27 g2(x)=g2(x)/(2*f*c*(1+x./t));
28 fplot(g1,[-0.35,6], 'LineWidth', 0.75);hold on;
29 g1 = text(1.25,2.5,'\leftarrowg1','FontSize',12,'Color','r');
30 fplot(g2,[-0.35,6], 'LineWidth',0.75); hold on;
31 g2 = text(2,1.8,'\leftarrowg2','FontSize',12,'Color','b');
32 xlabel('C'); ylabel('M');
33 %Plot x-axis and y-axis
34 xL = xlim;
35 yL = ylim;
36 line([0 0], yL, 'color', 'black'); %x-axis
37 line(xL, [0 0], 'color', 'black'); %y-axis
38
39 %plot the point condition E4
40 labels = {'E.4'};
```

```

41 plot(0,m/j, 'r.','MarkerSize',12); hold on ;
42 text(0,m/j,labels,'VerticalAlignment','top','HorizontalAlignment','right');
43
44 %Solve the system to get equilibrium points
45 syms z y x;
46     eqn1=a.*L-c.*y*x-g*x;
47     eqn2=p*(z+b.*x)./(1+z./t)-w.*x*y-f*y;
48     eqn3=j*y*z./(1+z./v)-m*z;
49     eqns=[eqn1==0,eqn2==0,eqn3==0];
50 [solx, soly, solz]=solve(eqns, [x,y,z]);
51 %Check whether those fixed points are real and positive
52 for i=1:length(solx)
53     o=floor(solz(i)); y=floor(solx(i)); r=floor(solz(i));
54     if isreal(o)==1 && isreal(y)==1 && isreal(r)==1
55         if floor(soly(i))>=0 && floor(solz(i))>=0 && floor(solx(i))>=0
56             Q(i)=solz(i);
57             W(i)=soly(i);
58         end
59     end
60 end
61
62 % CASE OF P INTERMEDIARY
63 % l={'E.1'};
64 % plot(Q(2),W(2),'r.','MarkerSize', 12); hold on;
65 % text(Q(2),W(2),l,'VerticalAlignment','top','HorizontalAlignment','left');
66 % l={'E.2'};
67 %le={'left'};
68 % plot(Q(3),W(3),'r.','MarkerSize', 12); hold on;
69 % text(Q(3),W(3),l,'VerticalAlignment','bottom','HorizontalAlignment',le);
70 % l={'E.3'};
71 %r={'right'};
72 % plot(Q(4),W(4),'r.','MarkerSize', 12); hold on;
73 % text(Q(4),W(4),l,'VerticalAlignment','bottom','HorizontalAlignment',r);
74
75 % %CASE OF P LOW
76 % l={'E.1'};
77 % plot(Q(5),W(5),'r.','MarkerSize', 12); hold on;
78 %r={'right'};
79 % text(Q(5),W(5),l,'VerticalAlignment','bottom','HorizontalAlignment',r);
80
81 %CASE OF P HIGH
82 l={'E.3'};
83 le={'left'};
84 plot(Q(2),W(2),'r.','MarkerSize', 12); hold on;
85 text(Q(2),W(2),l,'VerticalAlignment','bottom','HorizontalAlignment',le);
86 l={'E.1'};
87 r={'right'};
88 plot(Q(5),W(5),'r.','MarkerSize', 12); hold on;
89 text(Q(5),W(5),l,'VerticalAlignment','bottom','HorizontalAlignment',r);
90 end

```

```

1 function numericalconvergence
2 % This function plots the equilibrium points in all 3 cases, using the
3 % intersection of functions g1 and g2
4 %It plots as well the trajectories of many starting point and their kinetic
5 %trajectory to know the numerical stability of the equilibrium points
6 clear figure

```

```

7 lo=1.90;%L0
8 d=12.096;%LambdaL
9 a=d; %alphaL
10 b=0.05; %beta1
11 w=0.0120096; %alphaM
12 c=0.01; %alphaLox
13 g=2.0736; %LambdaLox
14 m=1.188; %Lambda2
15 j=2;%alpha2
16 t=1.4;%tau1
17 v=42/43;%tau2
18 f=1.9872;%LambdaM
19
20 syms x;
21 %p=1; % Low Permeability
22 p=5; %Intermediate Permeability
23 %p=7; %High Permeability
24
25 L=p*lo/(p+d); %Get L*
26 g1(x)=m*(1+x./v)./j;
27 g2(x)=((p*x*c-w*a*L*(1+x./t)-f*g*(1+x./t)) );
28 re=4*f*c*(1+x./t)*(p*x*g+p*a*L*b);
29 g2(x)=g2(x)+sqrt((p*x*c-w*a*L*(1+x./t)-f*g*(1+x./t))^2+re);
30 g2(x)=g2(x)/(2*f*c*(1+x./t));
31 fplot(g1,[-0.35,5.5], 'LineWidth', 0.75);hold on;
32 fplot(g2,[-0.35,5.5], 'LineWidth',0.75); hold on;
33 xlabel('C'); ylabel('M');
34
35 %Plot x-axis and y-axis
36 xL = xlim;
37 yL = ylim;
38 line([0 0], yL, 'color', 'black'); %x-axis
39 line(xL, [0 0], 'color', 'black'); %y-axis
40
41 labels = {'E.4'}; %plot the point condition E4
42 plot(0,m/j, 'r.','MarkerSize',12); hold on ;
43 text(0,m/j,labels,'VerticalAlignment','top','HorizontalAlignment','right');
44
45 %Solve the system to get equilibrium points
46 syms z y x;
47 eqn1=a.*L-c.*y*x-g*x;
48 eqn2=p*(z+b.*x)/(1+z./t)-w.*x*y-f*y;
49 eqn3=j*y*z./(1+z./v)-m*z;
50 eqns=[eqn1==0,eqn2==0,eqn3==0];
51 [solx, soly, solz]=solve(eqns, [x,y,z]);
52 %Check wether those fixed points are real and positive
53 for i=1:length(solx)
54 o=floor(solz(i)); y=floor(solx(i)); r=floor(solz(i));
55 if isreal(o)==1 && isreal(y)==1 && isreal(r)==1
56 if floor(soly(i))>=0 && floor(solz(i))>=0 && floor(solx(i))>=0
57 Q(i)=solz(i);
58 W(i)=soly(i);
59 end
60 end
61 end
62 % CASE OF P INTERMEDIARY
63 l={'E.1'};
64 plot(Q(2),W(2),'r.','MarkerSize', 12); hold on;
65 text(Q(2),W(2),l,'VerticalAlignment','top','HorizontalAlignment','left');

```

```

66 l={'E_2'};
67 le={'left'};
68 plot(Q(3),W(3),'r.','MarkerSize', 12); hold on;
69 text(Q(3),W(3),l,'VerticalAlignment','bottom','HorizontalAlignment',le);
70 l={'E_3'};
71 r={'right'};
72 plot(Q(4),W(4),'r.','MarkerSize', 12); hold on;
73 text(Q(4),W(4),l,'VerticalAlignment','bottom','HorizontalAlignment',r);
74
75 % %CASE OF P LOW
76 % l={'E_1'};
77 % plot(Q(5),W(5),'r.','MarkerSize', 12); hold on;
78 % r={'right'};
79 % text(Q(5),W(5),l,'VerticalAlignment','bottom','HorizontalAlignment',r);
80
81 % %CASE OF P HIGH
82 % l={'E_3'};
83 % le={'left'};
84 % plot(Q(2),W(2),'r.','MarkerSize', 12); hold on;
85 % text(Q(2),W(2),l,'VerticalAlignment','bottom','HorizontalAlignment',le);
86 % l={'E_1'};
87 % r={'right'};
88 % plot(Q(5),W(5),'r.','MarkerSize', 12); hold on;
89 % text(Q(5),W(5),l,'VerticalAlignment','bottom','HorizontalAlignment',r);
90
91 %Start Numerical Convergence
92 niter=50;
93 Δt=0.05;
94 u=zeros(7,4);
95 u(1,:)= [0.01,0.1,1.6,1.5];
96 u(2,:)= [0.2,0.02,0.7,3.5];
97 u(3,:)= [0.3,0.05,0.5,0.8];
98 u(4,:)= [0.1, 0.01,3 ,0.4];
99 u(5,:)= [0.02, 0.2, 0.95, 0.05];
100 u(6,:)= [0.2,0.01, 0.47, 0.18];
101 u(7,:)= [0.2,0.01, 0.55, 0.09];
102 [we ,n]=size(u);
103 for i=1:we
104     L0=u(i,1);
105     Lox0=u(i,2);
106     M0=u(i,3);
107     A0=u(i,4);
108     plot(A0,M0,'*');hold on;
109     for s=1:Δt:niter
110     L=L0+Δt*(p*(lo-L0)-d*L0);
111     Lox=Lox0+Δt*(a*L0-c*M0*Lox0-g*Lox0);
112     M=M0+Δt*(p*(A0+b*Lox0)/(1+A0/t)-w*M0*Lox0-f*M0);
113     A=A0+Δt*(j*M0*A0/(1+A0/v)-m*A0);
114     M0=M; A0=A; Lox0=Lox; L0=L;
115     plot(A0,M0,'k*','Markersize',0.5); hold on;
116     end
117     end
118     hold on
119     axis equal;
120     hold on
121     end

```

```

1  function Bifurcation
2  %This function allows us to plot the bifurcation diagram for values of the
3  %permeability p ranging from 0 to 8. Using the continuation method, we
4  %consider 2 different starting points followed by numerical trajectory.
5  %It allows to plot the concentration of M (stable equilibrium) in function
6  %of the permeability
7
8  %%Case 1
9  lo=1.90;%L0
10 d=12.096;%LambdaL
11 a=d; %alphaL
12 b=0.05; %beta1
13 w=0.0120096; %alphaM
14 c=0.01; %alphaLox
15 g=2.0736; %LambdaLox
16 m=1.188; %Lambda2
17 j=2;%alpha2
18 t=1.4;%taul
19 v=42/43;%tau2
20 f=1.9872;%LambdaM
21
22
23 %%Case 2
24 % lo=1.90;%L0
25 % d=12.096;%LambdaL
26 % a=d; %alphaL
27 % b=0.25; %beta1
28 % w=0.120096; %alphaM
29 % c=8; %alphaLox
30 % g=2.0736; %LambdaLox
31 % m=1.188; %Lambda2
32 % j=2;%alpha2
33 % t=1.4;%taul
34 % v=42/43;%tau2
35 % f=1.9872;%LambdaM
36
37
38 k=zeros(1,801); %The vector to be plotted containing for converged values
39 %of M
40 kl=zeros(1,801); %The vector to be plotted containing for converged values
41 % of Lox
42 p=zeros(1,801); % The permeability
43 p(1)=1;
44 for x=2:length(p)
45     p(x)=p(x-1)+0.01;
46 end
47 for y=1:1:length(p)
48     r=p(y);%Permeability
49     niter=5000;
50     dt=0.01;
51     u(1,:)=[0.04,4,5,4];
52     [we ,n]=size(u);
53     for i=1:we
54         L0=u(i,1);
55         Lox0=u(i,2);
56         M0=u(i,3);
57         A0=u(i,4);
58         for s=1:dt:niter
59             L=L0+dt*(r*(lo-L0)-d*L0);

```

```

60         Lox=Lox0+Δt*(a*L0-c*M0*Lox0-g*Lox0);
61         M=M0+Δt*(r*(A0+b*Lox0)/(1+A0/t)-w*M0*Lox0-f*M0);
62         A=A0+Δt*(j*M0*A0/(1+A0/v)-m*A0);
63         M0=M; A0=A; Lox0=Lox; L0=L;
64     end
65     k(1,y)=M0;
66     ki(1,y)=Lox0;
67 end
68 end
69 plot(p,k,'k-','LineWidth',1); hold on;
70 %plot(p,ki,'k-','LineWidth',1); hold on;
71
72 for y=1:1:length(p)
73     r=p(y);%Permeability
74     niter=5000;
75     Δt=0.01;
76     u(1,:)= [0.8, 1.4, 0.58, 0.0001];
77     [we ,n]=size(u);
78     for i=1:we
79         L0=u(i,1);
80         Lox0=u(i,2);
81         M0=u(i,3);
82         A0=u(i,4);
83         for s=1:Δt:niter
84             L=L0+Δt*(r*(lo-L0)-d*L0);
85             Lox=Lox0+Δt*(a*L0-c*M0*Lox0-g*Lox0);
86             M=M0+Δt*(r*(A0+b*Lox0)/(1+A0/t)-w*M0*Lox0-f*M0);
87             A=A0+Δt*(j*M0*A0/(1+A0/v)-m*A0);
88             %disp([L,Lox,M,A]);%pause;
89             M0=M; A0=A; Lox0=Lox; L0=L;
90         end
91         k(1,y)=M0;
92         ki(1,y)=Lox0;
93     end
94 end
95 plot(p,k,'k-','LineWidth',1); hold on;
96 %plot(p,ki,'k-','LineWidth',1); hold on;
97 end

```

```

1     function [C1 ,C2]=fun(p)
2     %This function computes the two condition C1 and C2, in function of the
3     %parameters
4
5     q=1.9;%L0
6     d=12.096;%LambdaL
7     a=d; %alphaL
8     b=0.05; %beta1
9     w=0.0120096; %alphaM
10    c=0.01; %alphaLox
11    g=2.0736; %LambdaLox
12    m=1.188; %Lambda2
13    j=2;%alpha2
14    t=1.4;%taul
15    v=42./43;%tau2
16    f=1.9872;%LambdaM
17
18    L=p*q/(p+d);

```

```

19 A=-c*f*m*m;
20 B=(-L*a*j*m*v*w+C*j*m*p*t*v-c*f*m*m*t-2*c*f*m*m*v-f*g*m*j*v)/(A);
21 C=(-L*a*j*m*t*v*w-L*a*j*m*v*v*w+C*j*m*p*t*v*v+g*j*j*p*t*v*v-2*c*f*m*m*t*v-c*f*m*m*v*v);
22 C=(C-g*f*j*m*t*v-f*g*j*m*v*v)/A;
23 D=(L*a*b*j*j*p*t*v*v-L*a*j*m*t*v*v*w-c*f*m*m*t*v*v-f*g*j*m*t*v*v)/A;
24 C1=4*B.^2-12*C;
25 C2=4/27.*D.*B.^3-1/27.*C.^2.*B.^2-2/3.*C.*B.*D+4/27.*C.^3+D.^2;
26
27 end

```

```

1 function Condition1
2 %This function provides where condition 1 is satisfied in function of the
3 %Permeability P, where all other parameters are taken as in Table 2.1
4 syms p;
5 [C1 ,C2]=fun(p);
6 eqn1=C1;
7 [solx]=solve(eqn1, [p]);
8 for i=1:length(solx)
9     y=floor(solx(i));
10    if isreal(y)==1
11        Q(i)=solx(i);
12    end
13 end
14
15 for i=1:length(Q)
16    plot(Q(i),0,'r.','MarkerSize', 12);hold on;
17 end
18 x0 = fzero(@(p) fun(p), -10.5);
19 x01 = fzero(@(p) fun(p), -11.5);
20 h1 = line([Q(1) Q(1)],[-4 10]); hold on;
21 h2 = line([Q(2) Q(2)],[-4 10]); hold on;
22 set([h1 h2], 'Color','k', 'LineWidth',2); hold on;
23
24 patch([-14 x01 x01 -14], [-4 -4 10 10],[1, 0.8, 0.8]); hold on;
25 patch([x0 6 6 x0], [-4 -4 10 10],[1, 0.8, 0.8]); hold on;
26 xL = [-14 6];
27 yL = [-4 10];
28 line([0 0], yL, 'color', 'black','LineWidth',1); %x-axis
29 line(xL, [0 0], 'color', 'black','LineWidth',1); %y-axis
30 end

```

```

1 function Condition2
2 %This function provides where condition 2 is satisfied in function of the
3 %Permeability P, where all other parameters are taken as in Table 2.1
4 syms p;
5 [C1 ,C2]=fun(p);
6 eqn1=C2;
7 [solx]=solve(eqn1, [p]);
8 for i=1:length(solx)
9     y=floor(solx(i));
10    if isreal(y)==1
11        Q(i)=solx(i);
12    end
13 end
14 for i=1:length(Q)

```

```

15     plot(Q(i),0,'r.','MarkerSize', 15);hold on;
16 end
17
18 x0 = fzero(@(p) fun1(p), -14.1);
19 x01 = fzero(@(p) fun1(p), -11);
20 x02 = fzero(@(p) fun1(p), 0.03);
21 x03 = fzero(@(p) fun1(p), 3.65);
22 h1 = line([Q(1) Q(1)],[-4 10]); hold on;
23 h2 = line([Q(2) Q(2)],[-4 10]); hold on;
24 h3 = line([Q(3) Q(3)],[-4 10]); hold on;
25 h4 = line([Q(6) Q(6)],[-4 10]); hold on;
26 set([h1 h2 h3 h4],'Color','k','LineWidth',0.5); hold on;
27 % %patch([x0-10 x0 x0 x0-10],[-1 -1 10 10],'o');
28 patch([-20 x0 x0 -20], [-4 -4 10 10],[0.8, 1, 0.8]); hold on;
29 patch([x01 x02 x02 x01], [-4 -4 10 10],[0.8, 1, 0.8]); hold on;
30 patch([x03 10 10 x03], [-4 -4 10 10],[1, 1, 0.6]); hold on;
31 xL = [-20 10];
32 yL = [-4 8];
33 line([0 0], yL, 'color', 'black','LineWidth',1); %x-axis
34 line(xL, [0 0], 'color', 'black','LineWidth',1); %y-axis
35 end

```